

Catalytic Reforming System Suitable for Transportation Applications

Majewski, Artur; Bossel, Ulf; Steinberger-Wilckens, Robert

DOI:

[10.1002/fuce.201700135](https://doi.org/10.1002/fuce.201700135)

License:

Other (please specify with Rights Statement)

Document Version

Peer reviewed version

Citation for published version (Harvard):

Majewski, A, Bossel, U & Steinberger-Wilckens, R 2018, 'Catalytic Reforming System Suitable for Transportation Applications', *Fuel Cells*. <https://doi.org/10.1002/fuce.201700135>

[Link to publication on Research at Birmingham portal](#)

Publisher Rights Statement:

This is the peer reviewed version of the following article: Majewski, A. J., Bossel, U. and Steinberger-Wilckens, R. (2018), Catalytic Reforming System Suitable for Transportation Applications. *Fuel Cells*, which has been published in final form at: <http://dx.doi.org/10.1002/fuce.201700135>. This article may be used for non-commercial purposes in accordance with Wiley Terms and Conditions for Use of Self-Archived Versions.

General rights

Unless a licence is specified above, all rights (including copyright and moral rights) in this document are retained by the authors and/or the copyright holders. The express permission of the copyright holder must be obtained for any use of this material other than for purposes permitted by law.

- Users may freely distribute the URL that is used to identify this publication.
- Users may download and/or print one copy of the publication from the University of Birmingham research portal for the purpose of private study or non-commercial research.
- User may use extracts from the document in line with the concept of 'fair dealing' under the Copyright, Designs and Patents Act 1988 (?)
- Users may not further distribute the material nor use it for the purposes of commercial gain.

Where a licence is displayed above, please note the terms and conditions of the licence govern your use of this document.

When citing, please reference the published version.

Take down policy

While the University of Birmingham exercises care and attention in making items available there are rare occasions when an item has been uploaded in error or has been deemed to be commercially or otherwise sensitive.

If you believe that this is the case for this document, please contact UBIRA@lists.bham.ac.uk providing details and we will remove access to the work immediately and investigate.



Catalytic Reforming System Suitable for Transportation Applications

Journal:	<i>Fuel Cells</i>
Manuscript ID	fuce.201700135.R1
Wiley - Manuscript type:	Original Research Paper
Date Submitted by the Author:	n/a
Complete List of Authors:	Majewski, Artur; University of Birmingham, School of Chemical Engineering Bossel, Ulf; ALMUS AG, Steinberger-Wilckens, Robert; University of Birmingham, Chemical Engineering
Keywords:	Solid Oxide Fuel Cells (SOFC), Liquefied Natural Gas (LNG), Partial Oxidation, Auxiliary Power Unit (APU), Fuel Cell System

SCHOLARONE™
Manuscripts

view

Catalytic Reforming System Suitable for Transportation

Applications

A.J. Majewski^{1*}, U. Bossel², R. Steinberger-Wilckens¹

¹ School of Chemical Engineering; University of Birmingham, Birmingham, B15 2TT, UK

²ALMUS AG, Morgenacherstrasse 2F, CH-5452, Oberrohrdorf, Switzerland

[*]Corresponding author: a.j.majewski@bham.ac.uk

Abstract

The paper describes operation and optimization of an onboard reforming system for an auxiliary power unit solid oxide fuel cell (SOFC APU) system for trucks that use liquid natural gas as fuel. The reformer system is based on partial oxidation and produces a reformat gas flow sufficient for a 100 W fuel cell. The ALMUS concept and configuration of the SOFC APU unit is described. The paper presents analyses of the efficiency of the partial oxidation reformer. The selected catalyst AB10 is analyzed under various reaction temperatures and molar ratios of CH₄:air. Two reforming reactor configurations are tested; both with 5 g of the catalyst. The optimal operating conditions for the reactor are proposed. The reformer is currently operated in an electric furnace that simulates the actual system and condition in a combustion chamber. The main focus is to obtain stable operation with high hydrogen yield and low coke deposition. The paper presents analyses of a 1,000 h partial oxidation stability test. The demonstration of the performance of the CPOX reformer confirms the system applicability. The observed slow catalyst deactivation is attributed to the detected coke deposition. The change to the structure of deposited coke along the reactor is explained.

Keywords: Solid Oxide Fuel Cells (SOFC), Liquefied Natural Gas (LNG), Partial Oxidation, Auxiliary Power Unit (APU), Fuel Cell System.

1 Introduction

Hydrogen as a fuel combined with fuel cells offers large potential benefits in reducing greenhouse gas and other emissions. The cost of hydrogen distribution and the lack of infrastructure are the main barriers to short-term large-scale implementation of hydrogen-based technologies. The current solution to this is distributed hydrogen production in small-scale portable (onboard) and stationary systems. Additional challenges are the fuel cell durability and reliability ^[1]. Economic analyses suggest that In early stages, distributed hydrogen production will be more cost-effective than a large scale centralized system ^[2]. Distributed reforming technology combined with fuel cells will promote decentralized energy production. Fuel cells have been undergoing rapid development in the last two decades and are becoming a practical choice that competes with batteries and combustion engines for domestic heat and power units, for grid backup power, or portable systems. To achieve long periods of operation, it is preferred to combine portable fuel cell applications directly with a reformer. Distributed reforming will deliver hydrogen where it would be needed. Such systems combine high-energy density of fuel with fuel cell high-power density. Reforming technologies are already available. However, to promote widespread introduction of distributed reforming, it is necessary to reduce cost by reducing reaction temperature, pressure, and materials cost (catalysts). Portable fuel cell applications include auxiliary power units (APU) (camping, caravans, etc.), light commercial applications (power for emergency, etc.), portable personal electronics (battery chargers, etc.), and support systems for transmission towers or telecommunication nodes ^[1].

For solid oxide fuel cells (SOFC), conversion of primary fuel to syngas can be achieved in an external reformer, directly in the fuel cell, or in indirect internal reforming. Internal reforming occurs directly on the anode or on the reformer that is separate, but upstream the anode ^[3]. However, to extend the cell life, external reforming of a minimum of 10% of hydrocarbons is required ^[4]. The risk for direct internal reforming is that coke deposition deactivates the

1
2
3 anode. An additional problem is temperature gradient formation caused by endothermic
4 reactions especially with higher hydrocarbons ^[5]. An alternative solution for a simple
5 reforming system is indirect internal reforming. In that system, the reforming catalyst is
6 located inside the fuel cell ^[5].
7
8

9
10
11 The fuel processor in which primary fuel is converted to hydrogen becomes integral to the
12 fuel cell stack. If the downstream fuel cell is sensitive to CO, additional fuel treatment and
13 purification is necessary. Usually, hydrogen production consists of several steps including
14 high temperature reforming on a catalyst followed by gas shift reaction to convert CO to CO₂
15 and at the same time increase H₂ output. The next step is the purification that depends on the
16 H₂ application. The growing interest in fuel cell technology has led to the development of a
17 variety of solutions for small-scale reforming systems and hydrogen production. Most
18 portable reforming systems combined with fuel cells concentrate on: methanol ^[6], ethanol ^[7],
19 and on propane ^[8] reforming. That is due to the high energy density and because fuel supply is
20 readily available and widely used for portable applications.
21
22

23
24 Reforming systems for portable applications require high efficiency, durability and rapid
25 start-up time ^[8]. From available reforming technologies for small scale reforming, steam
26 reforming, partial oxidation, and autothermal reforming are considered. The reforming system
27 has to be carefully selected from the available options for the specific application. Catalytic
28 partial oxidation (CPOX) is less energy efficient than is steam reforming or autothermal
29 reforming ^[6]. However, a heat exchanger is not required by this exothermic process and the
30 system is more compact. A partial oxidation reactor for portable reformers can be less
31 expensive than steam reforming ^[2] for systems feeding an SOFC. However, the amount of
32 added N₂ can increase the cost of purification for high purity hydrogen applications. The
33 advantage of partial oxidation is rapid start-up and system simplicity compared to steam
34 reforming. The disadvantage is the required high-pressure air pump. The start-up procedure
35 for a CPOX reactor consists of two steps: igniting/preheating and stabilizing time. Many
36
37
38
39
40
41
42
43
44
45
46
47
48
49
50
51
52
53
54
55
56
57
58
59
60

1
2
3 studies have been published about catalysts for partial oxidation of methane ^[9]. The reforming
4 catalyst usually has the structure of a packed bed or a monolith. The main CPOX reaction
5 produces carbon monoxide and hydrogen Eq. (1) but various other mechanisms are also
6 possible as detailed in Table 1.
7
8
9

10
11 The increasing number of liquefied natural gas (LNG) applications as a fuel for transportation
12 ^[10] opens the possibility for an onboard fuel cell application combined with methane
13 reforming. A major problem for trucks that use LNG is methane emissions related to boil-off
14 from the LNG tanks. LNG is composed primarily of methane (around 95%), but may also
15 contain some ethane, propane, nitrogen, and small quantities of higher hydrocarbons ^[11].
16
17

18 The purpose of the present paper is to examine the efficiency of partial oxidation reformers
19 for a 100 W portable SOFC system. In this work, the performance of the reforming system is
20 analyzed. The successful completion of this project will increase the potential for application
21 of portable (or onboard) fuel cell systems and will reduce methane emissions from LNG tanks
22 by utilization of boil-off gas.
23
24
25
26
27
28
29
30
31
32

33 34 **2 Experimental**

35 36 37 **2.1 APU system**

38
39 The tested reforming system is designed for a truck cab Auxiliary Power Unit designed by
40 ALMUS AG ^[12]. But it can also be adapted for any small-scale natural gas/CH₄ reforming
41 unit. When the truck engine is shut down, the truck's battery is fully charged, but will start to
42 discharge as the cab loads are operated, including lights, TV, computer, fridge, cab-heater fan,
43 etc. These loads will activate the fuel cell start-up sequence. It will take about 20 minutes to
44 warm up and will extract about 30 W of battery power to drive the fans and the electronics.
45
46 During fuel cell operation, the battery voltage reading will drive the fuel cell output. Before
47 the electricity generation from the fuel cell starts, some power is required to start the
48 reforming reaction and to heat-up the fuel cell stack, which comes from the truck battery. The
49
50
51
52
53
54
55
56
57
58
59
60

1
2
3 system will primarily use the boil-off LNG from the truck's tank. While the truck is in
4 motion, the LNG regasification occurs in a heat exchanger coupled to the engine exhaust.
5
6 During parking, if the inherent LNG boil-off in the tank is not sufficient to feed the SOFC
7 stack, an additional heat exchanger at the stack exhaust can be installed to obtain the required
8
9 NG feed. In the proposed system, the fuel processor reaches the required operating
10
11 temperature by combusting NG and air on a catalytic combustor. Once the device is hot, the
12
13 output from the reformer is fed to the fuel cell. The reforming reaction is self-sustained
14
15 without the addition of external fuel to the catalytic combustor. Two air pumps are needed for
16
17 the actual system: one for the CPOX reactor and the second for the cathode air. The exhaust
18
19 from the reformer is connected to the fuel cell (a planar fuel cell stack with 16 cells). The fuel
20
21 cell stack is equipped with an electric heater for the heat-up phase. ALMUS AG has shown
22
23 more recently, that special heating arrangements can provide a rapid starting planar stack,
24
25 which could be adapted for a truck cab APU, which needs to start in a few minutes^[13]. These
26
27 parts (16-cells stack, CPOX reformer, air preheater, air pump, air and fuel supply system, air
28
29 and fuel exhaust, valves, etc.) are closely packed, connected by pipes and valves and
30
31 surrounded by electric leads, thermocouples etc. to improve temperature distribution and
32
33 reduce the size of the APU unit. The SOFC-APU unit requires a DC-DC converter to reach
34
35 the 29 V charging level of the truck batteries.
36
37
38
39
40
41

42 **2.2 Reformer**

43
44 A small-scale reforming system has to be compact, simple and low cost. Partial oxidation was
45
46 chosen owing to the simple design and fast start-up, which makes it suitable for portable
47
48 power generation systems. A small CPOX reformer measuring 14.5 cm³ capable of producing
49
50 enough hydrogen for a 100 W size fuel cell was fabricated by ALMUS AG. On the CPOX
51
52 catalyst, NG is converted to hydrogen and carbon monoxide for the anode. The fuel
53
54 processing of the methane to produce hydrogen and carbon monoxide for the anode has been
55
56
57
58
59
60

1
2
3 proven in many tests. A range of catalysts was tested for partial oxidation of NG under
4
5 conditions typical for SOFC operation ^[5, 14]. For the experiments presented in this paper, the
6
7 AB10 catalyst was selected owing to its high activity and resistance to coke deposition; also
8
9 the CO yield was favorable for this catalyst. Characterization of the freshly prepared catalyst
10
11 was previously described ^[5, 14]. The exact composition of the catalyst and analyses of metal
12
13 particles sintering after the reaction cannot be disclosed due to proprietary reasons.

14
15 The partial oxidation reforming reaction was carried out in two fixed bed stainless-steel
16
17 reactors, each with 5 g of the catalyst: reactor (I) ALMUS AG 20 mm ID (with 6 mm gas
18
19 collection tube inside), and a tubular reactor (II) with a bed supported by porous ceramic, 10
20
21 mm ID. A tubular reactor with a bed supported by quartz wool was also tested. However, the
22
23 pressure in the reactor increased to 1.5 bar caused by the compaction of the wool as observed
24
25 after the experiment.

26
27
28 Mass flow controllers controlled the reactant flow rate (CH₄, air). The gas composition was
29
30 measured by a gas chromatograph after removing water from the reformat gas. The flow rate
31
32 of reformat was measured by a wet gas meter. The activity of the catalyst was studied by
33
34 temperature programmed reaction with a heating rate of 5°C min⁻¹ with highest temperature
35
36 650, 700 and 750°C under constant CH₄:air ratio (1:2.2, 1:2.4, 1:2.6 or 1:2.8) (CH₄ 724 mL
37
38 min⁻¹) and reaction pressure (1 atm). Small-scale portable units usually operate at close to
39
40 atmospheric pressure, small stand-alone reformers at a lower pressure of 2-3 atm, compared to
41
42 industrial-scale systems that operate at 15-25 atm ^[2].

43 44 45 46 47 **2.3 Experimental details**

48
49 The catalyst surface was characterised using a tabletop SEM Hitachi TM3030Plus.

50
51 The reactor external temperature was maintained at the constant temperature of 650, 700 or
52
53 750°C in a tubular furnace and monitored by thermocouples. The selected temperature range
54
55 represented the expected temperature of the afterburner zone of the ALMUS system ^[13] where
56
57 the reforming reactor is located.

1
2
3 The gas composition after the CPOX catalyst was analyzed using a mass spectrometer, MKS
4 Mini-Lab and gas chromatograph (Agilent Technologies 7890A) after cooling using an ice
5 trap. The gas chromatograph was equipped with seven columns, five valves and three
6
7 detectors: a flame ionization detector (FID) and two thermal conductivity detectors (TCD).
8
9
10 The combination of three packed columns (2x HayeSep Q and 1x Molsieve 5A) and two
11
12 valves were used for separation of CH₄, CO₂ and CO; a molecular sieve column was used for
13
14 H₂ separation.
15

16
17
18 The coke deposition was analyzed using temperature-dependent mass change profiles (TGA)
19
20 by a thermogravimetric analyzer Netzsch 209F1. The heating rate was 10°C min⁻¹, carried out
21
22 between room temperature and 1,000°C. Samples (10-20 mg) of the spent catalyst were
23
24 examined by the temperature programmed oxidation (TPO) method in air 50 mL min⁻¹. The
25
26 recorded mass reduction was attributed to carbon removal by oxidation.
27

28
29 The test equipment, all connections and gases were chosen to simulate the condition of the
30
31 SOFC APU system. The catalytic activity of the catalyst was evaluated by testing in methane
32
33 partial oxidation reforming in a continuous flow fixed bed reactor. Before reaction, the
34
35 catalyst was purged with nitrogen (1,000 mL min⁻¹) and heated to required temperature with a
36
37 rate of 5°C min⁻¹. Then a gas mixture of CH₄ and air was switched into the reactor. The partial
38
39 oxidation reforming reaction was carried out at a constant temperature of 650, 700 or 750°C.
40
41 Gas flow rates during all experiments were constant (CH₄ 724 mL min⁻¹) with CH₄:air molar
42
43 ratio of feed gases, respectively, 1:2.2 1:2.4 1:2.6 or 1:2.8. The experiment was conducted for
44
45 24 h (1,000 h for durability test). During the experiment, the exhaust gas composition was
46
47 continuously analyzed by the mass spectrometer and by GC in 30 min intervals.
48
49
50

51 **3 Results and Discussion**

52
53 The tested reformer is presented in Figure 1b. For the final design, the reformer is located
54
55 inside a catalytic combustor with an ignition system. The catalyst HiFUEL AB10 from
56
57
58
59
60

Johnson Matthey was tested for the system. The catalyst was deposited on alumina spheres of 2 mm diameter (Figure 1a). The catalyst (5 g) was located into the fix bed reactor; a stainless steel container (Figure 1b). The start-up procedure is still under investigation to optimize the required gas mixture proportions for the rapid start-up. In the actual system, the start-up procedure consists of two steps. The first is ignition and preheating of the reformer until it reaches around 450°C (above auto ignition or light-off temperature for the CH₄:air mixture over a Pt/Ru catalyst). The second is preheating of the fuel cell. In the presented report, start-up was simulated in the electric furnace. AB10 is a noble metal catalyst. Application of such catalyst makes sense for small-scale portable units where a small amount of catalyst is needed. The gas hourly space velocity (GHSV) was 30 L h⁻¹ g_{cat}⁻¹ and was lower than for indirect internal reforming tested in previous work [5]. According to literature [15], methane conversion is expected to be around 85-95%, at a temperature of 700-750°C, 1 bar, proportion CH₄:air in gas 1:2.4 and GHSV 30 L h⁻¹ g_{cat}⁻¹. Also partial oxidation thermodynamics predict high methane conversion for those reaction conditions [9a, 9c, 16].

Operating conditions of the tested reactor were optimized to generate syngas directly fed to the 100 W SOFC stack. When oxygen and methane are mixed a range of possible reactions can occur, which depend on the CH₄:air ratio, temperature, pressure and other conditions. A balance is required to produce the highest possible conversion to H₂ without C formation (coking). The reaction could be a combination of all the reactions listed in Table 1. The presence of ethane makes the NG partial oxidation more complex than partial oxidation of pure methane. A range of reactions is possible with ethylene and acetic acid as intermediate or final products. The goal of the optimization of the reactor design was to improve H₂ production and at the same time avoid carbon build-up.

The two reactor configurations (I and II) were tested for the partial oxidation reaction at identical conditions and with 5 g of the catalyst (Figure 2). Results obtained for the reformer (II) were similar to results for the reactor (I) developed by ALMUS. Therefore, this

1
2
3 configuration was used to test the system at various reaction conditions since the reactor (I)
4 for ALMUS was welded with no option to change the catalyst. The CH₄ conversion was
5 94.6% for the reactor (I) and 93.1% for the reactor (II) (average from 24 h reaction). A small
6
7 difference in catalyst selectivity to partial oxidation products was observed. For reactor (I), H₂
8 and CO₂ yields were slightly lower but CO yield was improved compared to reactor (II). This
9 suggests that dry reforming was more efficient in reactor (I). CO was formed with high
10 selectivity around 80%. H₂ selectivity was slightly lower, around 75% (Figure 2). Catalytic
11 activity for both reactors was stable during up to 24 h on stream. Verlato et al. [17] observed
12 that the dry reforming reaction Eq. (5) usually does not occur at a significant rate for noble
13 metal catalysts under partial oxidation conditions. It is possible that the gas collection tube
14 located inside the ALMUS reactor improved temperature distribution along the catalyst bed.
15 The temperature of the catalyst bed was not monitored. However, early results [5] confirmed
16 the formation of a hotspot around 5 mm from the reactor inlet with a temperature 50-70°C
17 above the external reactor temperature.

18
19
20
21
22
23
24
25
26
27
28
29
30
31
32
33 The AB10 catalyst was tested for partial oxidation of CH₄ under various reaction conditions
34 to optimize reforming. As shown in Figure 3, increasing reaction temperature improved
35 syngas production and methane conversion. H₂ and CO concentration increased with the
36 increase in reaction temperature. As expected, CH₄ conversion increased from 88% at 650°C
37 to 98% at 750°C. That was caused by the increase in efficiency of steam Eq. (4) and dry Eq.
38 (5) reforming reactions at the higher reaction temperature. H₂ yield increased from 52 to 82%
39 by increasing the reaction temperature from 650 to 750°C. However, increasing reaction
40 temperature above 650°C improved CH₄ conversion only slightly. The CO yield increased
41 with reaction temperature from 75% at 650°C to 82% at 750°C. The results received are
42 consistent with thermodynamic calculations [9a, 9c, 16]. The H₂ yield increased slightly for a
43 reaction temperature above 700°C. The fact that CO₂ flow increased from 16 to 21% at 700°C
44 and decreased to 14% when the temperature reached 750°C was caused by intensified water
45
46
47
48
49
50
51
52
53
54
55
56
57
58
59
60

1
2
3 gas shift reaction (3) and improved dry reforming (5). The high CO concentration at 750°C
4
5 resulted from endothermic steam and dry reforming and water gas shift reaction that shifts to
6
7 the left side of Eq. (3) at elevated temperature. Early results ^[5] suggested that the highest
8
9 operation temperature for the AB10 catalyst should be below 800°C. Coke deposition
10
11 increased above that temperature caused by CH₄ cracking.

12
13 Oxygen partial pressure affected the H₂ yield (Figure 4). Increasing the air partial pressure
14
15 improved CH₄ conversion and H₂ yield. According to modeling ^[18], for a ratio of CH₄:O₂
16
17 below 1 the primary products of the chemistry are products other than hydrogen, mostly CO,
18
19 CO₂ and H₂O. The molar ratio of CH₄:air 1:2.4 is close to the stoichiometric for the partial
20
21 oxidation reaction Eq. (1). Increasing or reducing that molar ratio influenced CH₄ conversion
22
23 Eq. (4). With a ratio of CH₄:O₂ above stoichiometric Eq. (1), there was not enough oxygen to
24
25 convert all methane. For lower CH₄:O₂ ratios, the active methane conversion region in the
26
27 catalyst bed increases in size ^[18]. However, increased amount of air mixed with methane
28
29 dilutes the fuel and increased GHSV. Also higher oxygen partial pressure results in CO and
30
31 H₂ combustion. The enhanced effect of the CH₄:air ratio could be also explained in terms of
32
33 different temperature profiles. The higher amount of oxygen is related to higher temperature
34
35 in the oxidation zone and, thus, faster reforming kinetics, despite the lower contact time
36
37 (higher GHSV).
38
39

40
41 In previous work ^[5] the same AB10 catalyst was tested for indirect internal reforming for a
42
43 100 W tubular SOFC system. However, in such design, there was a limitation to the catalyst
44
45 volume (GHSV 120 L h⁻¹ gcat⁻¹). For the external reforming reactor (for planar cells)
46
47 presented in this work, it was possible to operate at much lower GHSV of 30 L h⁻¹ gcat⁻¹. Fuel
48
49 had much longer contact time with the catalyst than for the system described previously ^[5].
50
51 The slower reactions of steam and dry reforming that follow the methane oxidation had
52
53 enough time to complete. That increased CH₄ conversion, reduced CO₂ production, and
54
55
56
57
58
59
60

1
2
3 improved CO and H₂ yield. For the CH₄:air ratio of 1:2.8 and 750°C, and the methane was
4
5 almost completely consumed.

6
7 For the tested reactor (fix bed, 5 g AB10 catalyst, CH₄ flow 724 mL min⁻¹), of all tested
8
9 conditions, CH₄:air 1:2.6 at 750°C was optimal for partial oxidation. At the optimum
10
11 conditions for CPOX, the catalytic durability of the catalyst was tested. The initial
12
13 concentration of CH₄, N₂ and O₂ at the reactor inlet was 27.8, 56.4 and 15.1%, respectively.
14
15 The catalytic activity of the AB10 catalyst under steady state conditions was evaluated at
16
17 750°C. The profile of the composition of the reformat gas is presented in Figure 5. The
18
19 syngas produced was diluted by N₂ (and Ar), with around 1.6 L min⁻¹ of N₂ at the reactor
20
21 exhaust. However, for some systems, dilution by N₂ can increase cell performance by
22
23 improving the temperature distribution along the cell [5, 14]. Degradation in hydrogen yield was
24
25 around 10% after 1,000 h of partial oxidation under steady state operation, from 900 to 795
26
27 mL min⁻¹. CO yield decreased from 450 to 405 mL min⁻¹ after 1,000 h of reaction. The
28
29 production of CO₂ slowly increased during the 1,000 h testing. The CH₄ concentration at the
30
31 reactor exhaust also increased from around 3 to more than 20 mL min⁻¹. The total increase in
32
33 CO₂ and CH₄ flow rate was the same as the decrease in CO flow. The decrease in the
34
35 hydrogen flow rate was related to the CO decrease (2.5:1) and to the CO₂ and CH₄ increase
36
37 (also 2.5:1). That was close to the stoichiometry of the steam reforming reaction. This
38
39 suggests that steam reforming is the major reaction in the reforming zone of the reactor.
40
41
42 Deactivation of the tested catalyst affected the reforming activity of steam and dry reforming
43
44 reactions. The possible reason for deactivation of the noble metal catalyst tested was coke
45
46 deposition. However, even after 1,000 h, the CH₄ concentration was below 1%, as shown in
47
48 Figure 5. CH₄ conversion decreased from 99 to 94% after 1,000 h operation (Figure 6). With
49
50 this rate of degradation in catalyst activity, the reactor should operate with high efficiency for
51
52 a minimum of 5,000 h. No oxygen was observed at the reactor exhaust for all tested cases. In
53
54
55
56
57
58
59
60

1
2
3 partial oxidation, oxygen is consumed in the first few millimeters of the catalyst bed by
4 surface reactions ^[18].

5
6
7 Figure 7 shows SEM images of the AB10 catalyst after the 1,000 h reaction experiment. The
8 surface of the catalyst particles becomes smoother after 1,000 h caused by sintering, except at
9 the reactor inlet where particles were covered by coke flakes (Figure 7a-b). Debris of Fe from
10 oxidation of the stainless-steel reactor were visible on the surface of the catalyst particles after
11 the reaction, caused by the size of the reactor (10 mm ID). The structure of deposited coke at
12 the reactor inlet differed from the rest of the reactor. At the inlet, coke had a structure of
13 flakes (Figure 7b-c) agglomerated in big particles. The catalyst in the middle of the reactor
14 and at the exhaust was coated with small coke particles equally distributed on the catalyst
15 surface Figure 7e-f).

16
17
18 The deposited coke is a significant component of catalyst deactivation. Deposited carbon
19 along the catalyst bed was analyzed by TGA. The coke deposition was much lower than
20 expected. Early results ^[5] for the AB10 catalyst suggested that lack of oxygen leads to coke
21 formation on the CPOX catalyst. The used CH₄:air molar ratio of 1:2.6 presenter in this report
22 is close to stoichiometric and could result in high coke deposition on the CPOX catalyst.
23
24 However, a lower GHSV with higher reaction temperature and a different catalyst form
25 (spheres) improved resistance to coke deposition. The amount of deposited coke decreased
26 with the catalyst length (Table 2). The inlet is the most active part of the catalyst bed. Beretta
27 et al. ^[19] reported that 93% of methane can be converted within the first 5 mm from the
28 catalyst inlet during partial oxidation. Higher coke deposition in the inlet zone was detected
29 despite the fact that presence of oxygen should prevent this. This might be explained by
30 different type of deposited coke with the inlet displaying the graphitic type, while the
31 amorphous type prevailed further downstream the reactor. The characteristic of deposited
32 coke changed along the catalyst bed. For samples of the catalyst from the reactor inlet, the
33 change of mass at 680°C was caused by coke oxidation. The high oxidation temperature
34
35
36
37
38
39
40
41
42
43
44
45
46
47
48
49
50
51
52
53
54
55
56
57
58
59
60

1
2 suggests graphite-like carbon. However, samples from the middle had a change of mass at
3
4 100–150°C caused by moisture removal and a slow steady linear reduction of mass between
5
6 300 and 1,000°C. Samples of the catalyst from the reactor outlet (after moisture removal at
7
8 100–150°C) had a slow linear change of mass between 300 and 600°C, after that temperature
9
10 the mass was stable. This suggests, that at the bed exhaust soft carbon was deposited
11
12 (probably on the metal sites) and mixed graphite and soft coke deposited in the middle of the
13
14 reactor. Shamsi et al. ^[20] suggested that coke formed on the support is less reactive than coke
15
16 deposited on metal sites. This may suggest that oxygen present in the reactant gas mixture at
17
18 the catalyst bed inlet oxidizes hydrogen from the deposited coke making it more graphitic.
19
20 The slow deactivation of the catalyst with time can be related to the detected coke deposition.
21
22 Coke deposition decreased with the catalyst length. The color of the catalyst changed after the
23
24 reaction. Fresh catalyst was brown. After 1,000 h of partial oxidation at 750°C, all particles of
25
26 the catalyst at the reactor inlet (up to 2 cm from inlet) turned white, and particles in the middle
27
28 and at the outlet black.
29
30
31
32 The catalyst deactivation was caused by coke deposition combined with sintering. During
33
34 partial oxidation, there is always a hot-spot formation at the reactor inlet. The hot-spot
35
36 formation has been reported ^[17, 19] to result in progressive loss of the catalyst activity that
37
38 might result in a faster deactivation of the catalyst. Such loss strongly influences the rate of
39
40 methane reforming reactions. According to literature ^[17], increase in the particle size of noble
41
42 metal is the most probable reason for the decrease in partial oxidation performance during
43
44 long time tests. Noble metal sintering affects reforming reactions Eqs. (4) and (5) but has a
45
46 lesser effect on oxidation Eqs. (1) and (2) ^[17]. The AB10 is a noble metal catalyst and it can
47
48 be regenerated by coke oxidation. The procedure for cyclic oxidation to guarantee the long-
49
50 term operation is still under investigation. The regeneration temperature and time is limited by
51
52 the portable application of the tested system. TPO analyses of the catalyst used suggest that
53
54 the regeneration temperature should be above 600°C; however, it should be below system
55
56
57
58
59
60

1
2
3 operation temperature. To prevent coke accumulation in long-term operation, Lee et al. [8]
4 suggested the cyclic operation of several hours of partial oxidation with few minutes of air
5 oxidation. The cyclic operation can reduce the rate of catalyst deactivation. However, for a
6 system where reformat is connected directly to an SOFC, that solution is not practical.
7
8 The presented results are based on simulation of LNG. In the final system, the low fuel
9 temperature (down to -160°C) will reduce the catalyst activity at the reformer inlet and will
10 lead to a smoother temperature profile. Fuel unconverted on the catalyst will be afterward
11 converted on the anode. That can lead to a cooling effect on the SOFC fuel inlet and is
12 currently being studied. The investigation of fuel dilution by N_2 from partial oxidation is also
13 still ongoing. The obtained results suggest that the final system control needs a mechanism
14 that will stop the flow of air in case of problems with fuel supply to prevent anode oxidation.
15
16
17
18
19
20
21
22
23
24
25
26

27 **4 Conclusions**

28
29 The performance of a small reforming system for a 100 W SOFC system was evaluated. The
30 catalyst AB10 was analyzed under various reaction temperatures and CH_4 :air molar ratios.
31
32 Although the amount of deposited coke was small, after 1,000 hours of operation the catalyst
33 slowly deactivated with the decrease in CH_4 conversion from 99 to 94% after 1,000 hours of
34 operation. The demonstrated performance of the CPOX reformer confirmed the potential for
35 application of the proposed reformer in an auxiliary power system. It is expected, that the
36 reformer tested in this study will be integrated with a 100 W SOFC system, targeting a market
37 for auxiliary power systems for LNG-powered trucks.
38
39
40
41
42
43
44
45
46
47

48 **Acknowledgements**

49
50 The results are part of the SAFARI project funded under Europe's Fuel Cell and Hydrogen
51 Joint Undertaking (FCH JU), Grant Agreement No.325323. The Consortium gratefully
52 acknowledges the support of the FCH JU.
53
54
55
56
57
58
59
60

References

- [1] T. Wilberforce, A. Alaswad, A. Palumbo, M. Dassisti, A. G. Olabi, *Int. J. Hydrogen Energy* **2016**, *41*, 16509-16522.
- [2] J. M. Ogden, can be fund under <http://www.afdc.energy.gov/pdfs/31948.pdf>, **2002**, pp. 1-52.
- [3] P. Aguiar, D. Chadwick, L. Kershenbaum, *Chem. Eng. Sci.* **2002**, *57*, 1665-1677.
- [4] Q. Fang, L. Blum, P. Batfalsky, N. H. Menzler, U. Packbier, D. Stolten, *Int. J. Hydrogen Energy* **2013**, *38*, 16344-16353.
- [5] A. J. Majewski, A. Dhir, *J. Electrochem. Soc.* **2016**, *163*, F272-F277.
- [6] H.-S. Wang, K.-Y. Huang, Y.-J. Huang, Y.-C. Su, F.-G. Tseng, *Appl. Energy* **2015**, *138*, 21-30.
- [7] T. Aicher, J. Full, A. Schaadt, *Int. J. Hydrogen Energy* **2009**, *34*, 8006-8015.
- [8] S. Lee, G. Keskar, C. Liu, W. R. Schwartz, C. S. McEnally, J.-Y. Kim, L. D. Pfefferle, G. L. Haller, *Appl. Catal. B* **2012**, *111-112*, 157-164.
- [9] **a**A. A.-S. Saleh, *Open Catal. J.* **2013**, *6*, 17-28; **b**Q. Zhu, X. Zhao, Y. Deng, *J. Nat. Gas Chem.* **2004**, *13*, 191-203; **c**B. C. Enger, R. Lødeng, A. Holmen, *Appl. Catal. A:* **2008**, *346*, 1-27.
- [10] **a**E. Stefana, F. Marciano, M. Alberti, *J. Loss Prev. Process Ind.* **2016**, *39*, 39-58; **b**Q. Tang, J. Fu, J. Liu, F. Zhou, Z. Yuan, Z. Xu, *Appl. Therm. Eng.* **2016**, *103*, 1351-1361; **c**O. Schinas, M. Butler, *Ocean Eng.* **2016**, *122*, 84-96.
- [11] E. Graham, A. Kenbar, *Flow Meas. Instrum.* **2015**, *44*, 79-88.
- [12] ALMUS AG, can be fund under <http://www.almus-ag.ch/>, **2016**.
- [13] **a**U. Bossel, *ECS Trans.* **2015**, *68*, 193-199; **b**U. Bossel, in *12th European SOFC and SOE forum*, Lucerne, **2016**.
- [14] A. J. Majewski, A. Dhir, *ECS Trans.* **2015**, *68*, 2189-2198.

- 1
2
3 [15] aP. D. F. Vernon, M. L. H. Green, A. K. Cheetham, A. T. Ashcroft, *Catal. Lett.* **1990**,
4 6, 181-186; bV. Dal Santo, C. Mondelli, V. De Grandi, A. Gallo, S. Recchia, L.
5 Sordelli, R. Psaro, *Appl. Catal. A* **2008**, 346, 126-133.
6
7
8
9 [16] aS. Kumar, S. Kumar, J. K. Prajapati, *Int. J. Hydrogen Energy* **2009**, 34, 6655-6668;
10 bJ. E. P. Navalho, I. Frenzel, A. Loukou, J. M. C. Pereira, D. Trimis, J. C. F. Pereira,
11 *Int. J. Hydrogen Energy* **2013**, 38, 6989-7006.
12
13
14
15 [17] E. Verlato, S. Barison, S. Cimino, F. Dergal, L. Lisi, G. Mancino, M. Musiani, L.
16 Vázquez-Gómez, *Int. J. Hydrogen Energy* **2014**, 39, 11473-11485.
17
18
19 [18] A. Raoufi, S. Kapadia, J. C. Newman Iii, *Comput. Chem. Eng.* **2016**, 93, 266-283.
20
21
22 [19] A. Beretta, A. Donazzi, D. Livio, M. Maestri, G. Groppi, E. Tronconi, P. Forzatti,
23 *Catal. Today* **2011**, 171, 79-83.
24
25
26 [20] A. Shamsi, J. P. Baltrus, J. J. Spivey, *Appl. Catal. A* **2005**, 293, 145-152.
27
28
29
30
31
32
33
34
35
36
37
38
39
40
41
42
43
44
45
46
47
48
49
50
51
52
53
54
55
56
57
58
59
60

Figure Captions

Figure 1: A - catalyst HiFUEL AB10 - pellets. B - External reformer (I) for planar cells (designed and manufactured by ALMUS AG).

Figure 2: CH₄ conversion and products yields from different reactors (average from 24 h reaction): (I) - ALMUS reactor; (II) - tubular reactor with ceramic support. Reaction at 700°C, CH₄:air 1:2.4, AB10 catalyst 5 g, CH₄ 724 mL min⁻¹.

Figure 3: Reactor (II) performance at the different reaction temperature (average from 24 h). CH₄:air 1:2.4, 5 g AB10 catalyst, CH₄ gas-in flow 724 mL min⁻¹.

Figure 4: Reactor (II) performance for different CH₄:air ratio 1:x (average from 24 h). Reaction temperature 700°C, 5 g AB10 catalyst CH₄ if flow 724 mL min⁻¹.

Figure 5: Change of gas composition at the reactor (II) outlet with time. Partial oxidation CH₄:air 1:2.6, at 750°C, AB10 catalyst 5 g with GHSV 150 L h⁻¹ g_{cat}⁻¹.

Figure 6: Change in methane conversion with time. Partial oxidation CH₄:air 1:2.6, at 750°C, AB10 catalyst 5 g with GHSV 150 L h⁻¹ g_{cat}⁻¹, reactor (II).

Figure 7: SEM scans of the AB10 spent catalyst after 1,000 h at 750°C with GHSV 150 L h⁻¹ g_{cat}⁻¹, CH₄:air 1:2.6, reactor (I), A-C reactor inlet, D-F reactor exhaust. C and F - EDX carbon mapping of scans B and E respectively.

1
2
3 **Table Captions**
4

5 Table 1. Overall reactions in the methane partial oxidation system

ΔH_{298}°	Reaction	Name	Equation Number (as referred in manuscript)
-36 kJ mol ⁻¹	$2CH_4 + O_2 \rightarrow 2CO + 4H_2$	CH ₄ partial oxidation	(1)
-802 kJ mol ⁻¹	$CH_4 + 2O_2 \rightarrow CO_2 + 2H_2O$	CH ₄ combustion	(2)
-41 kJ mol ⁻¹	$CO + H_2O \leftrightarrow CO_2 + H_2$	water gas shift	(3)
+206 kJ mol ⁻¹	$CH_4 + H_2O \leftrightarrow CO + 3H_2$	CH ₄ steam reforming	(4)
+247 kJ mol ⁻¹	$CH_4 + CO_2 \leftrightarrow 2CO + 2H_2$	CH ₄ dry reforming	(5)
-131 kJ mol ⁻¹	$CO + H_2 \leftrightarrow C + H_2O$	CO hydrogenation	(6)
+75 kJ mol ⁻¹	$CH_4 \leftrightarrow C + 2H_2$	CH ₄ cracking	(7)
-173 kJ mol ⁻¹	$2CO \leftrightarrow CO_2 + C$	Boudouard	(8)
-282 kJ mol ⁻¹	$2CO + O_2 \rightarrow 2CO_2$	CO oxidation	(9)
-241 kJ mol ⁻¹	$2H_2 + O_2 \rightarrow 2H_2O$	H ₂ oxidation	(10)

Table 2. Coke deposition on AB10 catalyst - TGA. Catalyst after 1,000 h at 750°C with GHSV 150 L h⁻¹ g_{cat}⁻¹, CH₄:air 1:2.6

Position in reactor	Coke / mg g _{cat} ⁻¹
Inlet	14.8
Middle	12.8
Outlet	6.0

For Peer Review



Figure 1: A - catalyst HiFUEL AB10 - pellets. B - External reformer (I) for planar cells (designed and manufactured by ALMUS AG).

60x39mm (300 x 300 DPI)

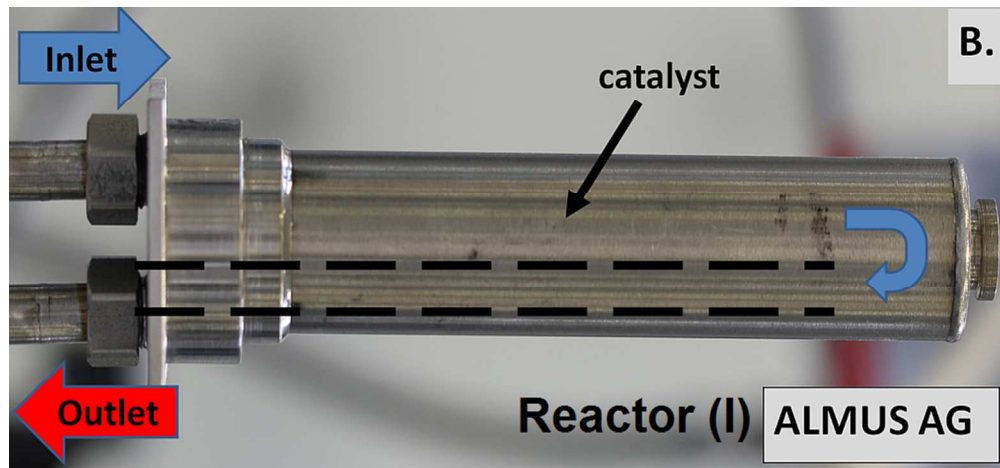


Figure 1: B

85x39mm (300 x 300 DPI)

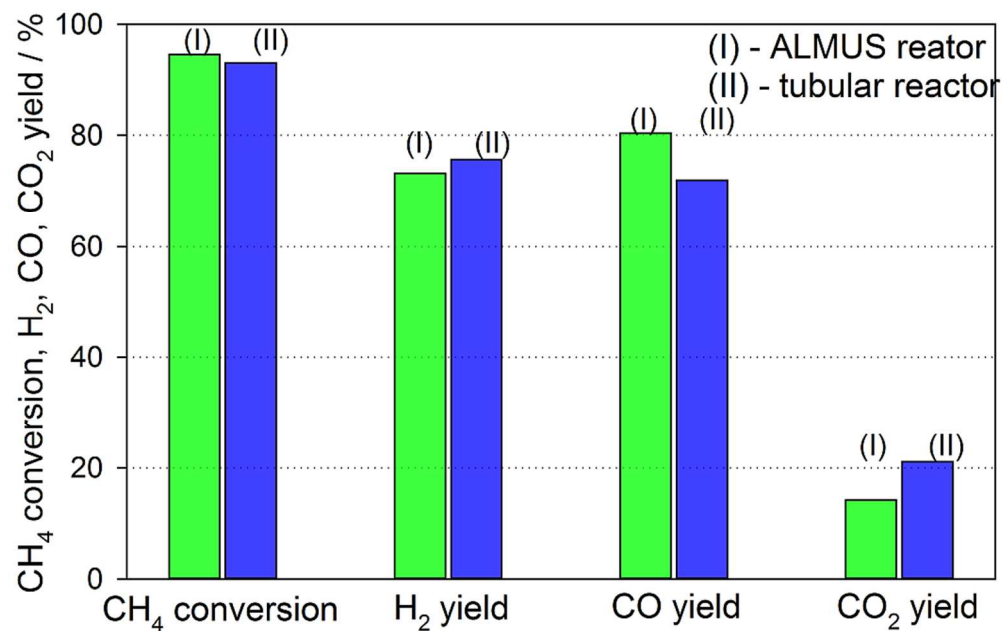


Figure 2: CH₄ conversion and products yields from different reactors (average from 24 h reaction): (I) - ALMUS reactor; (II) - tubular reactor with ceramic support. Reaction at 700°C, CH₄:air 1:2.4, AB10 catalyst 5 g, CH₄ 724 mL min⁻¹.

90x57mm (300 x 300 DPI)

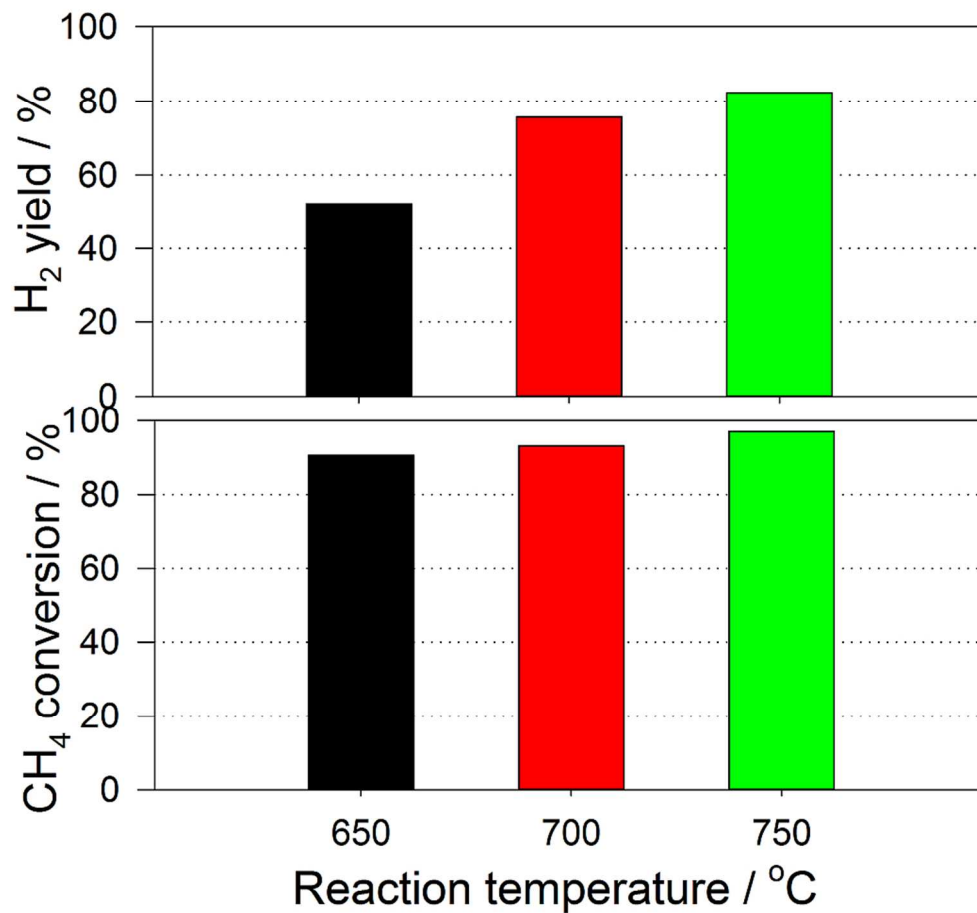


Figure 3: Reactor (II) performance at the different reaction temperature (average from 24 h). CH₄:air 1:2.4, 5 g AB10 catalyst, CH₄ gas-in flow 724 mL min⁻¹.

90x82mm (300 x 300 DPI)

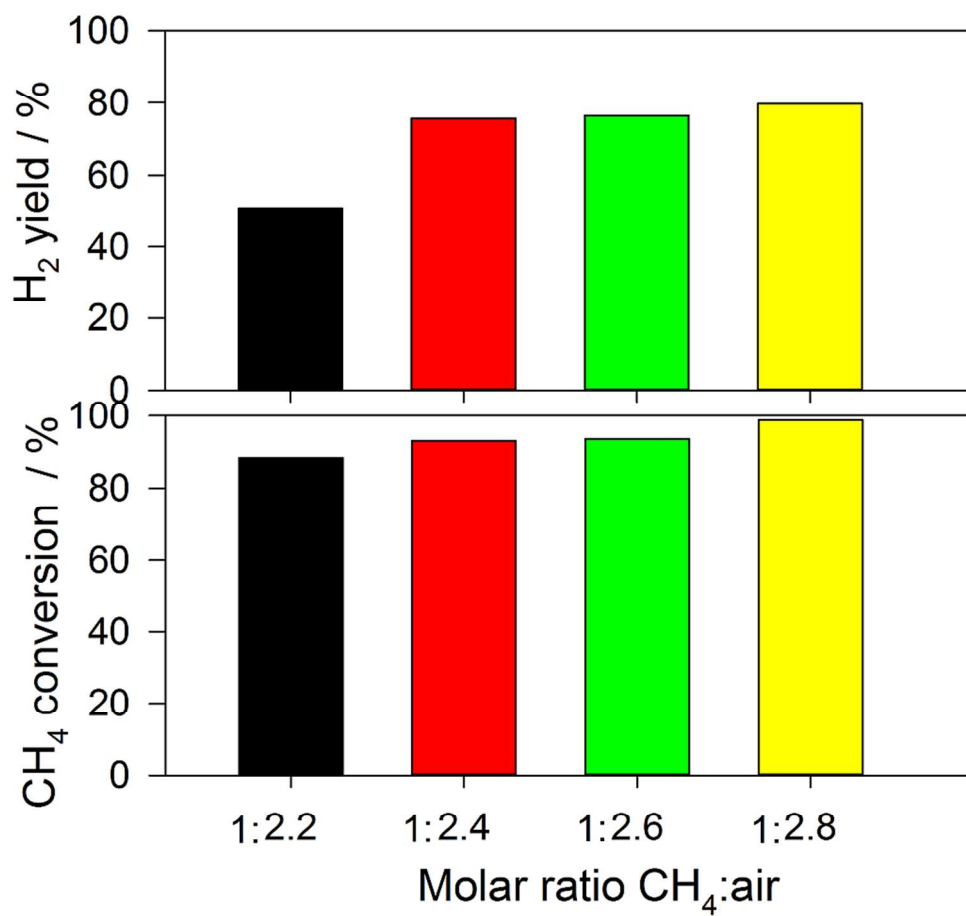


Figure 4: Reactor (II) performance for different CH₄:air ratio 1:x (average from 24 h). Reaction temperature 700°C, 5 g AB10 catalyst CH₄ if flow 724 mL min⁻¹.

90x83mm (300 x 300 DPI)

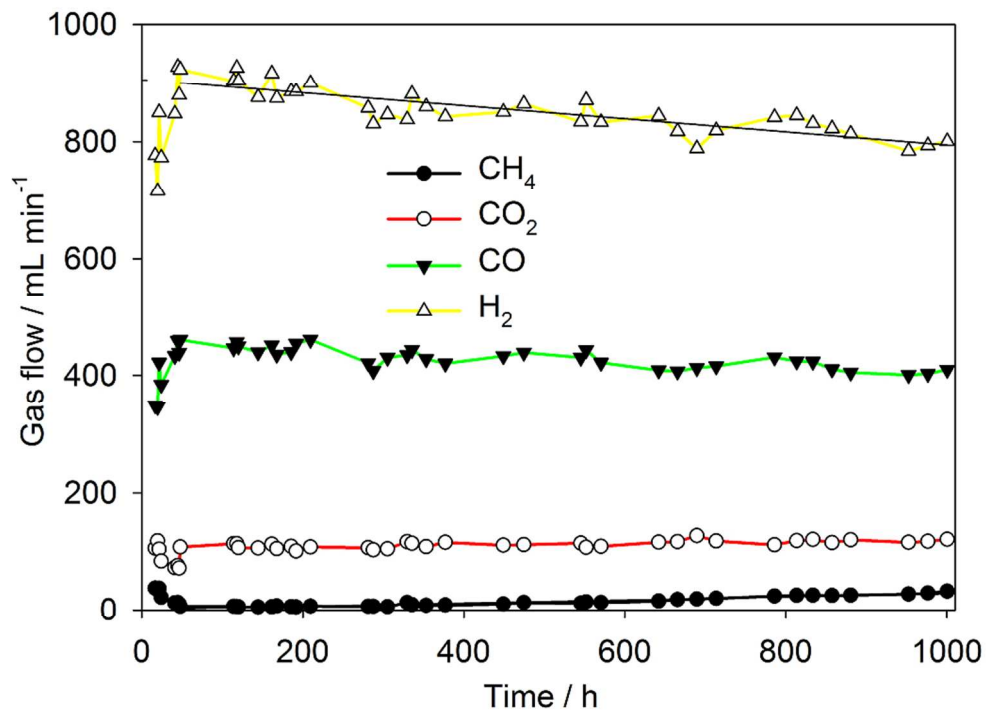


Figure 5: Change of gas composition at the reactor (II) outlet with time. Partial oxidation CH₄:air 1:2.6, at 750°C, AB10 catalyst 5 g with GHSV 150 L h⁻¹ gcat⁻¹.

90x66mm (300 x 300 DPI)

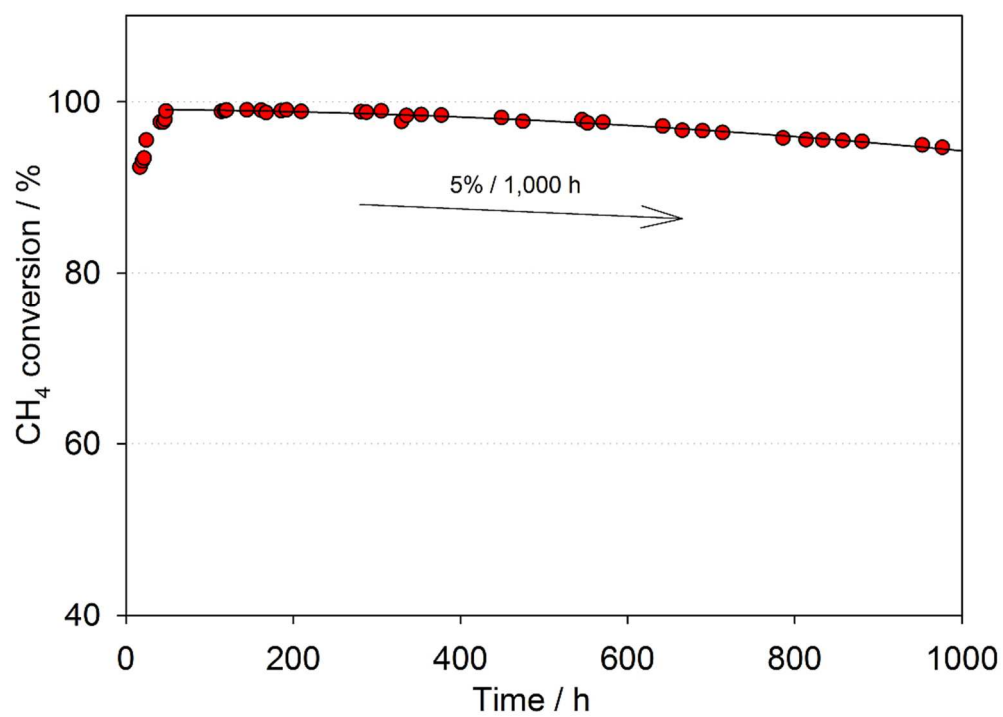
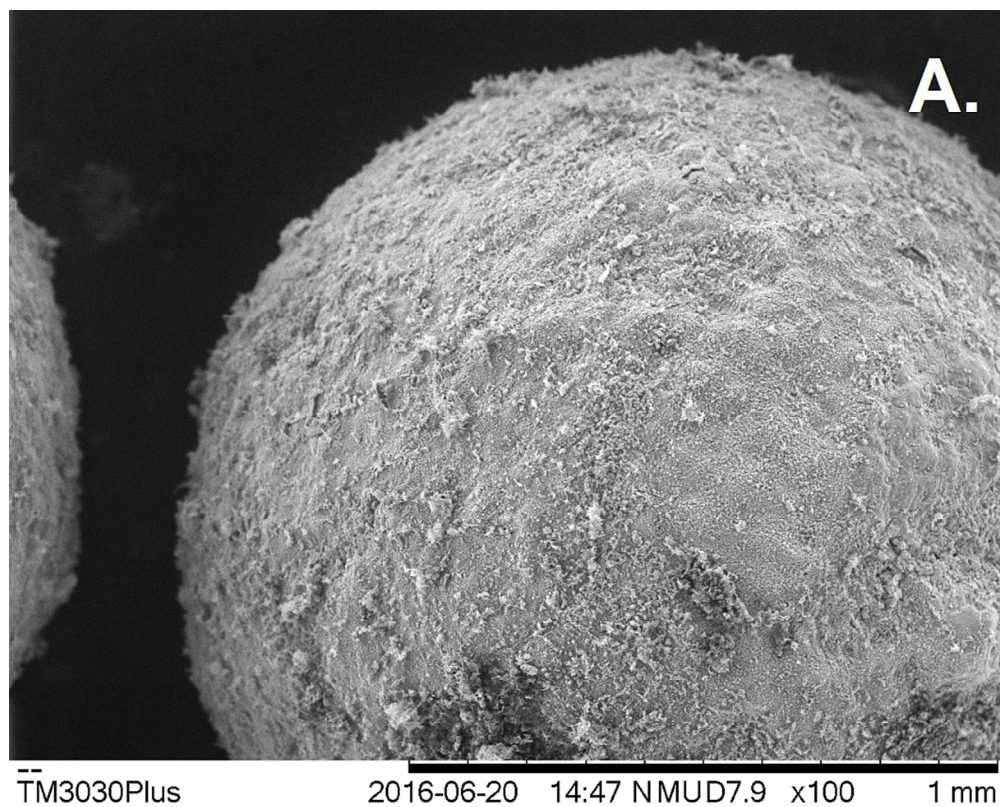


Figure 6: Change in methane conversion with time. Partial oxidation CH₄:air 1:2.6, at 750oC, AB10 catalyst 5 g with GHSV 150 L h⁻¹ gcat⁻¹, reactor (II).

90x65mm (300 x 300 DPI)



33 Figure 7: SEM scans of the AB10 spent catalyst after 1,000 h at 750oC with GHSV 150 L h⁻¹ gcat⁻¹, CH₄:air
34 1:2.6, reactor (I), A-C reactor inlet, D-F reactor exhaust. C and F - EDX carbon mapping of scans B and E
35 respectively.

36 90x73mm (300 x 300 DPI)

37
38
39
40
41
42
43
44
45
46
47
48
49
50
51
52
53
54
55
56
57
58
59
60

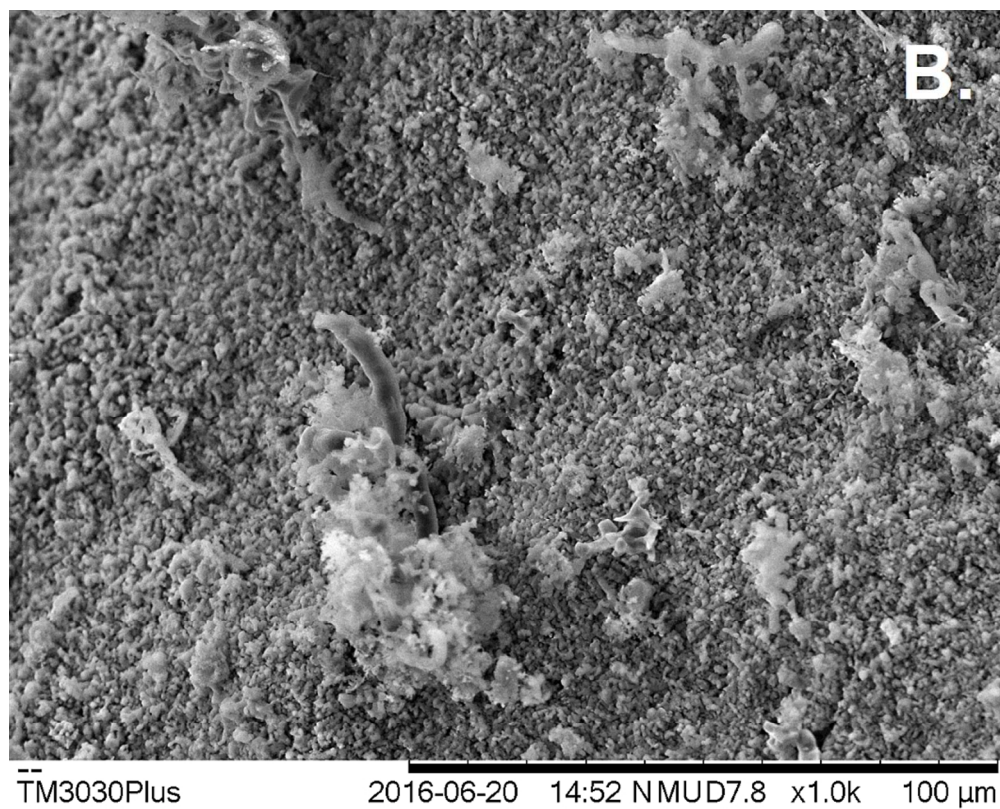


Figure 7: B

90x73mm (300 x 300 DPI)

1
2
3
4
5
6
7
8
9
10
11
12
13
14
15
16
17
18
19
20
21
22
23
24
25
26
27
28
29
30
31
32
33
34
35
36
37
38
39
40
41
42
43
44
45
46
47
48
49
50
51
52
53
54
55
56
57
58
59
60

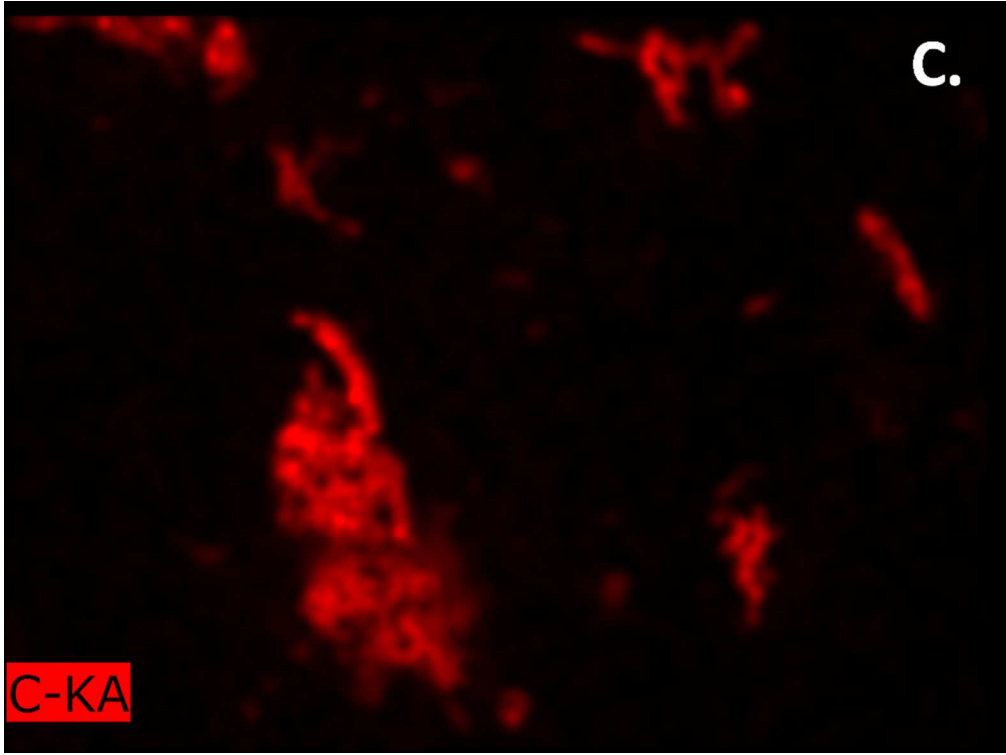


Figure: 7C
90x67mm (300 x 300 DPI)

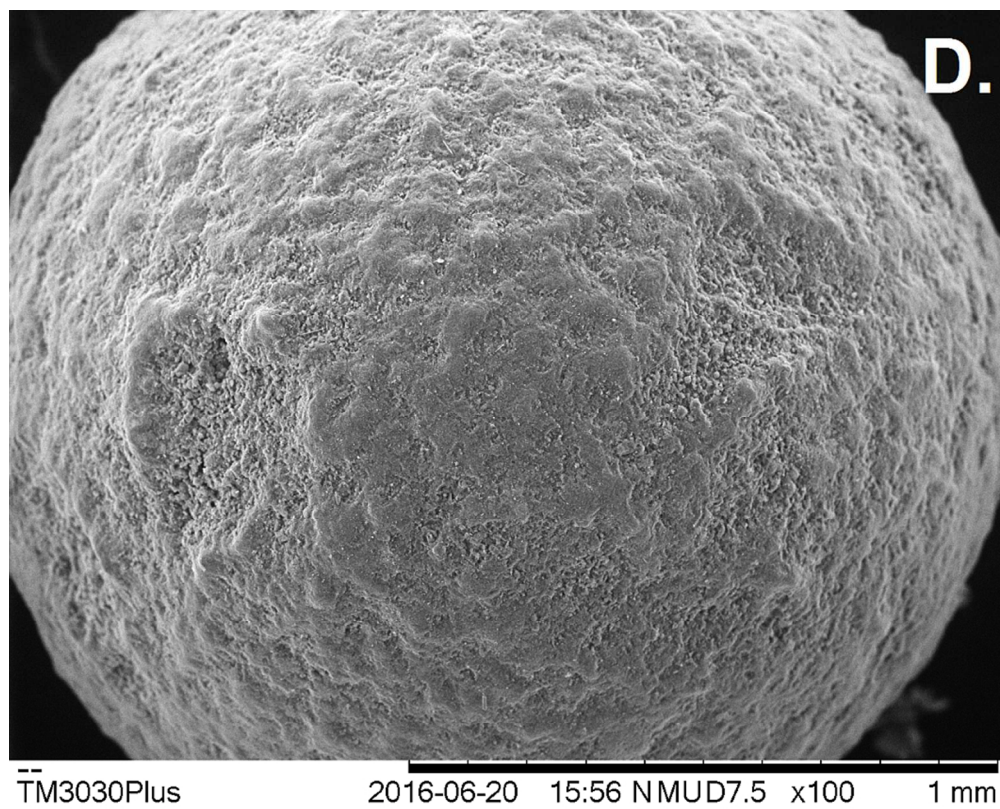


Figure: 7D

90x73mm (300 x 300 DPI)

1
2
3
4
5
6
7
8
9
10
11
12
13
14
15
16
17
18
19
20
21
22
23
24
25
26
27
28
29
30
31
32
33
34
35
36
37
38
39
40
41
42
43
44
45
46
47
48
49
50
51
52
53
54
55
56
57
58
59
60

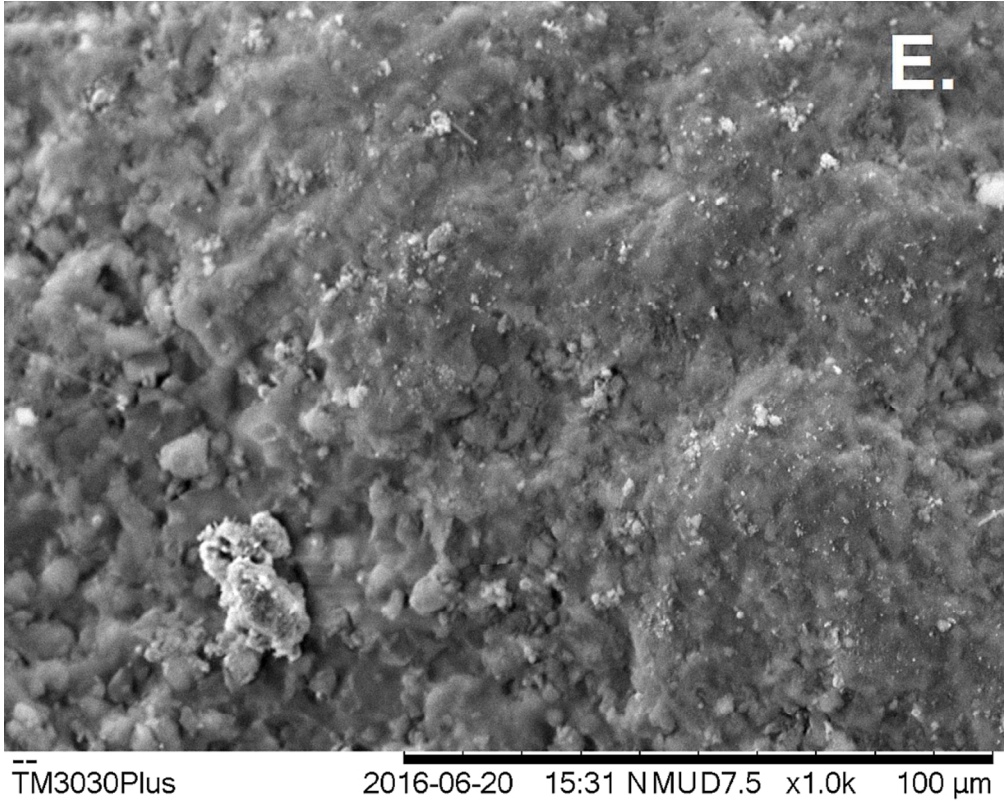


Figure: 7E
90x73mm (300 x 300 DPI)

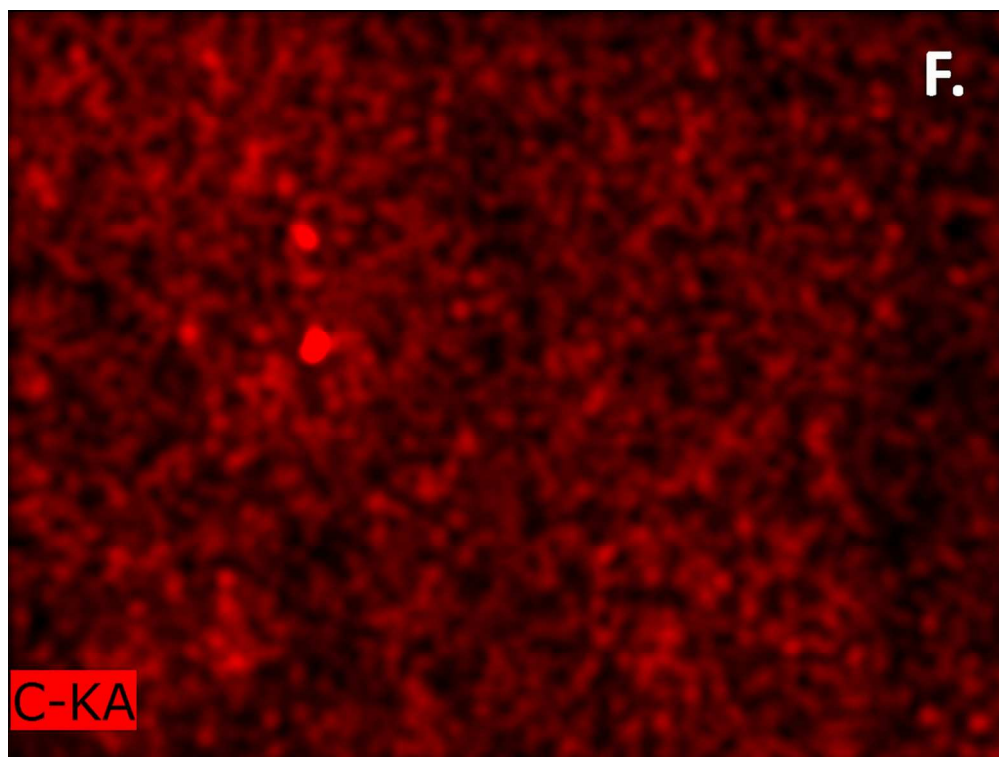


Figure: 7F

90x67mm (300 x 300 DPI)

Catalytic Reforming System Suitable for Transportation Applications

A.J. Majewski^{1*}, U. Bossel², R. Steinberger-Wilckens¹

¹ School of Chemical Engineering; University of Birmingham, Birmingham, B15 2TT, UK,

²ALMUS AG, Morgenacherstrasse 2F, CH-5452, Oberrohrdorf, Switzerland

*Corresponding author: a.j.majewski@bham.ac.uk

Abstract

The paper describes operation and optimization of an onboard reforming system for an auxiliary power unit solid oxide fuel cell (SOFC APU) system for trucks that use liquid natural gas as fuel. The reformer system is based on partial oxidation and produces a reformat gas flow sufficient for a 100 W fuel cell. The ALMUS concept and configuration of the SOFC APU unit is described. The paper presents analyses of the efficiency of the partial oxidation reformer. The selected catalyst AB10 is analyzed under various reaction temperatures and molar ratios of CH₄:air. Two reforming reactor configurations are tested; both with 5 g of the catalyst. The optimal operating conditions for the reactor are proposed. The reformer is ~~currently~~ operated in an electric furnace that simulates the actual system and condition in a combustion chamber. The main focus is to obtain stable operation with high hydrogen yield and low coke deposition. The paper presents analyses of a 1,000 h partial oxidation stability test. The demonstration of the performance of the CPOX reformer confirms the system applicability. The observed slow catalyst deactivation is attributed to the detected coke deposition. The change to the structure of deposited coke along the reactor is explained.

Keywords: Solid Oxide Fuel Cells (SOFC), Liquefied Natural Gas (LNG), Partial Oxidation, Auxiliary Power Unit (APU), Fuel Cell System

1 Introduction

Hydrogen as a fuel combined with fuel cells offers large potential benefits in reducing greenhouse gas and other emissions. The cost of hydrogen distribution and the lack of infrastructure are the main barriers to short-term large-scale implementation of hydrogen-based technologies. The current solution to this is distributed hydrogen production in small-scale portable (onboard) and stationary systems. Additional challenges are the fuel cell durability and reliability ^[1]. Economic analyses suggest that in early stages, distributed hydrogen production will be more cost-effective than a large scale centralized system ^[2]. Distributed reforming technology combined with fuel cells will promote decentralized energy production. Fuel cells have been undergoing rapid development in the last two decades and are becoming a practical choice that competes with batteries and combustion engines for domestic heat and power units, for grid backup power, or portable systems. To achieve long periods of operation, it is preferred to combine portable fuel cell applications directly with a reformer. Distributed reforming will deliver hydrogen where it would be needed. Such systems combine high-energy density of fuel with fuel cell high-power density. Reforming technologies are already available. However, to promote widespread introduction of distributed reforming, it is necessary to reduce cost by reducing reaction temperature, pressure, and materials cost (catalysts). Portable fuel cell applications include auxiliary power units (APU) (camping, caravans, etc.), light commercial applications (power for emergency, etc.), portable personal electronics (battery chargers, etc.), and support systems for transmission towers or telecommunication nodes ^[1].

For solid oxide fuel cells (SOFC), conversion of primary fuel to syngas can be achieved in an external reformer, directly in the fuel cell, or in indirect internal reforming. Internal reforming occurs directly on the anode or on the reformer that is separate, but upstream the anode ^[3]. However, to extend the cell life, external reforming of a minimum of 10% of hydrocarbons is required ^[4]. The risk for direct internal reforming is that coke deposition deactivates the anode. An additional problem is temperature gradient formation caused by endothermic reactions especially with higher

hydrocarbons^[5]. An alternative solution for a simple reforming system is indirect internal reforming. In that system, the reforming catalyst is located inside the fuel cell^[5].

The fuel processor in which primary fuel is converted to hydrogen becomes integral to the fuel cell stack. If the downstream fuel cell is sensitive to CO, additional fuel treatment and purification is necessary. Usually, hydrogen production consists of several steps including high temperature reforming on a catalyst followed by gas shift reaction to convert CO to CO₂ and at the same time increase H₂ output. The next step is the purification that depends on the H₂ application. The growing interest in fuel cell technology has led to the development of a variety of solutions for small-scale reforming systems and hydrogen production. Most portable reforming systems combined with fuel cells concentrate on: methanol^[6], ethanol^[7], and on propane^[8] reforming. That is due to the high energy density and because fuel supply is readily available and widely used for portable applications. Reforming systems for portable applications require high efficiency, durability and rapid start-up time^[8]. From available reforming technologies for small scale reforming, steam reforming, partial oxidation, and autothermal reforming are considered. The reforming system has to be carefully selected from the available options for the specific application. Catalytic partial oxidation (CPOX) is less energy efficient than is steam reforming or autothermal reforming^[6]. However, a heat exchanger is not required by this exothermic process and the system is more compact. A partial oxidation reactor for portable reformers can be less expensive than steam reforming^[2] for systems feeding an SOFC. However, the amount of added N₂ can increase the cost of purification for high purity hydrogen applications. The advantage of partial oxidation is rapid start-up and system simplicity compared to steam reforming. The disadvantage is the required high-pressure air pump. The start-up procedure for a CPOX reactor consists of two steps: igniting/preheating and stabilizing time. ~~There are m~~Many studies have been published about catalysts for partial oxidation of methane^[9]. The reforming catalyst usually has the structure of a packed bed or a monolith. The main CPOX reaction produces carbon monoxide and hydrogen Eq. (1) but various other mechanisms are also possible as detailed in Table 1.

The increasing number of liquefied natural gas (LNG) applications as a fuel for transportation^[10] opens the possibility for an onboard fuel cell application combined with methane reforming. A major problem for trucks that use LNG is methane emissions related to boil-off from the LNG tanks. LNG is composed primarily of methane (around 95%), but may also contain some ethane, propane, nitrogen, and small quantities of higher hydrocarbons^[11].

The purpose of the present paper is to examine the efficiency of partial oxidation reformers for a 100 W portable SOFC system. In this work, the performance of the reforming system is analyzed. The successful completion of this project will increase the potential for application of portable (or onboard) fuel cell systems and will reduce methane emissions from LNG tanks by utilization of boil-off gas.

2 Experimental details

2.1 APU system

The tested reforming system is designed for a truck cab Auxiliary Power Unit designed by ALMUS AG^[12]. But it can also be adapted for any small-scale natural gas/CH₄ reforming unit. When the truck engine is shut down, the truck's battery is fully charged, but will start to discharge as the cab loads are operated, including lights, TV, computer, fridge, cab-heater fan, etc. These loads will activate the fuel cell start-up sequence. It will take about 20 minutes to warm up and will extract about 30 W of battery power to drive the fans and the electronics. During fuel cell operation, the battery voltage reading will drive the fuel cell output. Before the electricity generation from the fuel cell starts, some power is required to start the reforming reaction and to heat-up the fuel cell stack, which comes from the truck battery. The system will primarily use the boil-off LNG from the truck's tank. While the truck is in motion, the LNG regasification takes placeoccurs in a heat exchanger coupled to the engine exhaust. During parking, if the inherent LNG boil-off in the tank is not sufficient to feed the SOFC stack, an additional heat exchanger at the stack exhaust can be installed to obtain the required

1
2
3 NG feed. In the proposed system, the fuel processor reaches the required operating temperature by
4 combusting NG and air on a catalytic combustor. Once the device is hot, the output from the
5 reformer is fed to the fuel cell. The reforming reaction is self-sustained without the addition of
6 external fuel to the catalytic combustor. Two air pumps are needed for the actual system: one for
7 the CPOX reactor and the second for the cathode air. The exhaust from the reformer is connected to
8 the fuel cell (a planar fuel cell stack with 16 cells). The fuel cell stack is equipped with an electric
9 heater for the heat-up phase. ALMUS AG has shown more recently, that special heating
10 arrangements can provide a rapid starting planar stack, which could be adapted for a truck cab APU,
11 which needs to start in a few minutes^[13]. These parts (16-cells stack, CPOX reformer, air preheater,
12 air pump, air and fuel supply system, air and fuel exhaust, valves, etc.) are closely packed, connected
13 by pipes and valves and surrounded by electric leads, thermocouples etc. to improve temperature
14 distribution and reduce the size of the APU unit. The SOFC-APU unit requires a DC-DC converter to
15 reach the 29 V charging level of the truck batteries.
16

17 2.2 Reformer

18 A small-scale reforming system has to be compact, simple and low cost. Partial oxidation was chosen
19 ~~due-owing~~ to the simple design and fast start-up, which makes it suitable for portable power
20 generation systems. A small CPOX reformer measuring 14.5 cm³ capable of producing enough
21 hydrogen for a 100 W size fuel cell was fabricated by ALMUS AG. On the CPOX catalyst, NG is
22 converted to hydrogen and carbon monoxide for the anode. The fuel processing of the methane to
23 produce hydrogen and carbon monoxide for the anode has been proven in many tests. A range of
24 catalysts was tested for partial oxidation of NG under conditions typical for SOFC operation^[5, 14]. For
25 the experiments presented in this paper, the AB10 catalyst was selected ~~due-owing~~ to its high
26 activity and resistance to coke deposition; also the CO yield was favorable for this catalyst.
27 Characterization of the freshly prepared catalyst was previously described^[5, 14]. The exact
28 composition of the catalyst and analyses of metal particles sintering after the reaction cannot be
29 disclosed due to proprietary reasons.
30

31 The partial oxidation reforming reaction was carried out in two fixed bed stainless-steel reactors,
32 ~~both-each~~ with 5 g of the catalyst: reactor (I) ALMUS AG 20 mm ID (with 6 mm gas collection tube
33 inside), and a tubular reactor (II) with a bed supported by porous ceramic, 10 mm ID. A tubular
34 reactor with a bed supported by quartz wool was also tested. However, the pressure in the reactor
35 increased to 1.5 bar ~~due-caused by~~ the compaction of the wool as observed after the experiment.
36 Mass flow controllers controlled the reactant flow rate (CH₄, air). The gas composition was measured
37 by a gas chromatograph after removing water from the reformat gas. The flow rate of reformat
38 was measured by a wet gas meter. The activity of the catalyst was studied by temperature
39 programmed reaction with a heating rate of 5°C min⁻¹ with highest temperature 650, 700 and 750°C
40 under constant CH₄:air ratio (1:2.2, 1:2.4, 1:2.6 or 1:2.8) (CH₄ 724 mL min⁻¹) and reaction pressure (1
41 atm). Small-scale portable units usually operate at close to atmospheric pressure, small stand-alone
42 reformers at a lower pressure of 2-3 atm, compared to industrial-scale systems that operate at 15-25
43 atm^[2].
44

45 2.3 Experimental details

46 The catalyst surface was characterised using a tabletop SEM Hitachi TM3030Plus.

47 The reactor external temperature was maintained at the constant temperature of 650, 700 or 750°C
48 in a tubular furnace and monitored by thermocouples. The selected temperature range represented
49 the expected temperature of the afterburner zone of the ALMUS system^[13] where the reforming
50 reactor is located.
51

52 The gas composition after the CPOX catalyst was analyzed using a mass spectrometer, MKS Mini-Lab
53 and gas chromatograph (Agilent Technologies 7890A) after cooling ~~by-passing-through~~ using an ice
54 trap. The gas chromatograph was equipped with seven columns, five valves and three detectors: a
55 flame ionization detector (FID) and two thermal conductivity detectors (TCD). The combination of
56
57
58
59
60

three packed columns (2x HayeSep Q and 1x Molsieve 5A) and two valves were used for separation of CH₄, CO₂ and CO; a molecular sieve column was used for H₂ separation.

The coke deposition was analyzed using temperature-dependent mass change profiles (TGA) by a thermogravimetric analyzer Netzsch 209F1. The heating rate was 10°C min⁻¹, carried out between room temperature and 1,000°C. Samples (10-20 mg) of the spent catalyst were examined by the temperature programmed oxidation (TPO) method in air 50 mL min⁻¹. The recorded mass reduction was attributed to carbon removal by oxidation.

The test equipment, all connections and gases were chosen to simulate the condition of the SOFC APU system. The catalytic activity of the catalyst was evaluated by testing in methane partial oxidation reforming in a continuous flow fixed bed reactor. Before reaction, the catalyst was purged with nitrogen (1,000 mL min⁻¹) and heated to required temperature with a rate of 5°C min⁻¹. Then a gas mixture of CH₄ and air was switched into the reactor. The partial oxidation reforming reaction was carried out at a constant temperature of 650, 700 or 750°C. Gas flow rates during all experiments were constant (CH₄ 724 mL min⁻¹) with CH₄:air molar ratio of feed gases, respectively, 1:2.2 1:2.4 1:2.6 or 1:2.8. The experiment was conducted for 24 h (1,000 h for durability test). During the experiment, the exhaust gas composition was continuously analyzed by the mass spectrometer and by GC in 30 min intervals.

3 Results and discussion

The tested reformer is presented in Figure 1b. For the final design, the reformer is located inside a catalytic combustor with an ignition system. The catalyst HiFUEL AB10 from Johnson Matthey was tested for the system. The catalyst was deposited on alumina spheres of 2 mm diameter (Figure 1a). The catalyst (5 g) was located into the fix bed reactor; a stainless- steel container (Figure 1b). The start-up procedure is still under investigation to optimize the required gas mixture proportions for the rapid start-up. In the actual system, the start-up procedure consists of two steps. The first is ignition and preheating of the reformer until it reaches around 450°C (above auto ignition or light-off temperature for the CH₄:air mixture over a Pt/Ru catalyst). The second is preheating of the fuel cell. In the presented report, start-up was simulated in the electric furnace. AB10 is a noble metal catalyst. Application of such catalyst makes sense for small-scale portable units where a small amount of catalyst is needed. The gas hourly space velocity (GHSV) was 30 L h⁻¹ g_{cat}⁻¹ and was lower than for indirect internal reforming tested in previous work^[5]. According to literature^[15], methane conversion is expected to be around 85-95%, at a temperature of 700-750°C, 1 bar, proportion CH₄:air in gas 1:2.4 and GHSV 30 L h⁻¹ g_{cat}⁻¹. Also partial oxidation thermodynamics predict high methane conversion for those reaction conditions^[9a, 9c, 16].

Operating conditions of the tested reactor were optimized to generate syngas directly fed to the 100 W SOFC stack. When oxygen and methane are mixed a range of possible reactions can occur, which depend on the CH₄:air ratio, temperature, pressure and other conditions. A balance is required to produce the highest possible conversion to H₂ without C formation (coking). The reaction could be a combination of all the reactions listed in Table 1. The presence of ethane makes the NG partial oxidation more complex than partial oxidation of pure methane. A range of reactions is possible with ethylene and acetic acid as intermediate or final products. The goal of the optimization of the reactor design was to improve H₂ production and at the same time avoid carbon build-up.

The two reactor configurations (I and II) were tested for the partial oxidation reaction at identical conditions and with 5 g of the catalyst (Figure 2). Results obtained for the reformer (II) were similar to results for the reactor (I) developed by ALMUS. Therefore, this configuration was used to test the system at various reaction conditions since the reactor (I) for ALMUS was welded with no option to change the catalyst. The CH₄ conversion was ~~(I)~~ 94.6% for the reactor (I) and ~~(II)~~ 93.1% for the reactor (II) (average from 24 h reaction) ~~respectively. There was a~~ small difference in catalyst selectivity to partial oxidation products was observed. For reactor (I), H₂ and CO₂ yields were slightly lower but CO yield was improved compared to reactor (II). This suggests that dry reforming was more efficient in reactor (I). CO was formed with high selectivity around 80%. H₂ selectivity was

1
2
3 slightly lower, around 75% (Figure 2). Catalytic activity for both reactors was stable during up to 24 h
4 on stream. Verlató et al. ^[17] observed that the dry reforming reaction Eq. (5) usually does not occur
5 at a significant rate for noble metal catalysts under partial oxidation conditions. It is possible that the
6 gas collection tube located inside the ALMUS reactor improved temperature distribution along the
7 catalyst bed. The temperature of the catalyst bed was not monitored. However, ~~initial-early~~ results ^[5]
8 confirmed the formation of a hotspot around 5 mm from the reactor inlet with a temperature 50-
9 70°C above the external reactor temperature.

10 The AB10 catalyst was tested for partial oxidation of CH₄ under various reaction conditions to
11 optimize reforming. As shown in Figure 3, increasing reaction temperature improved syngas
12 production and methane conversion. H₂ and CO concentration increased with the increase in
13 reaction temperature. As expected, CH₄ conversion increased from 88% at 650°C to 98% at 750°C.
14 That was caused by the increase in efficiency of steam Eq. (4) and dry Eq. (5) reforming reactions at
15 the higher reaction temperature. H₂ yield increased from 52 to 82% by increasing the reaction
16 temperature from 650 to 750°C. However, increasing reaction temperature above 650°C improved
17 CH₄ conversion only slightly. The CO yield increased with reaction temperature from 75% at 650°C to
18 82% at 750°C. The results received are consistent with thermodynamic calculations ^[9a, 9c, 16]. The H₂
19 yield increased slightly for a reaction temperature above 700°C. The fact that CO₂ flow increased
20 from 16 to 21% at 700°C and decreased to 14% when the temperature reached 750°C ~~was caused~~
21 ~~by due to intensified increased~~ water gas shift reaction (3) and improved dry reforming (5). The high
22 CO concentration at 750°C resulted from endothermic steam and dry reforming and water gas shift
23 reaction that shifts to the left side of Eq. (3) at elevated temperature. Early results ^[5] suggested that
24 the highest operation temperature for the AB10 catalyst should be below 800°C. Coke deposition
25 increased above that temperature caused by CH₄ cracking.

26 Oxygen partial pressure affected the H₂ yield (Figure 4). Increasing the air partial pressure improved
27 CH₄ conversion and H₂ yield. According to modeling ^[18], for a ratio of CH₄:O₂ below 1 the primary
28 products of the chemistry are products other than hydrogen, mostly CO, CO₂ and H₂O. The molar
29 ratio of CH₄:air 1:2.4 is close to ~~the~~ stoichiometric for the partial oxidation reaction Eq. (1).
30 Increasing or reducing that molar ratio ~~obviously~~ influenced CH₄ conversion Eq. (4). With a ratio of
31 CH₄:O₂ above stoichiometric Eq. (1), there was not enough oxygen to convert all methane. For lower
32 CH₄:O₂ ratios, the active methane conversion region in the catalyst bed increases in size ^[18].
33 However, increased amount of air mixed with methane dilutes the fuel and increased GHSV. Also
34 higher oxygen partial pressure results in CO and H₂ combustion. The enhanced effect of the CH₄:air
35 ratio could be also explained in terms of different temperature profiles. The higher amount of
36 oxygen is related to higher temperature in the oxidation zone and, thus, faster reforming kinetics,
37 despite the lower contact time (higher GHSV).

38 In previous work ^[5] the same AB10 catalyst was tested for indirect internal reforming for a 100 W
39 tubular SOFC system. However, in such design, there was a limitation to the catalyst volume (GHSV
40 120 L h⁻¹ gcat⁻¹). For the external reforming reactor (for planar cells) presented in this work, it was
41 possible to operate at much lower GHSV of 30 L h⁻¹ gcat⁻¹. Fuel had much longer contact time with
42 the catalyst than for the system described previously ^[5]. The slower reactions of steam and dry
43 reforming that follow the methane oxidation had enough time to complete. That increased CH₄
44 conversion, reduced CO₂ production, and improved CO and H₂ yield. For the CH₄:air ratio of 1:2.8 and
45 750°C, and the methane was almost completely consumed.

46 For the tested reactor (fix bed, 5 g AB10 catalyst, CH₄ flow 724 mL min⁻¹), of all tested conditions,
47 CH₄:air 1:2.6 at 750°C was optimal for partial oxidation. At the optimum conditions for CPOX, the
48 catalytic durability of the catalyst was tested. The initial concentration of CH₄, N₂ and O₂ at the
49 reactor inlet was 27.8, 56.4 and 15.1%, respectively. The catalytic activity of the AB10 catalyst under
50 steady state conditions was evaluated at 750°C. The profile of the composition of the reformaté gas
51 is presented in Figure 5. The syngas produced was diluted by N₂ (and Ar), with around 1.6 L min⁻¹ of
52 N₂ at the reactor exhaust. However, for some systems, dilution by N₂ can increase cell performance
53 by improving the temperature distribution along the cell ^[5, 14]. Degradation in hydrogen yield was
54
55
56
57
58
59
60

1
2
3 around 10% after 1,000 h of partial oxidation under steady state operation, from 900 to 795 mL min⁻¹.
4 CO yield decreased from 450 to 405 mL min⁻¹ after 1,000 h of reaction. The production of CO₂
5 slowly increased during the 1,000 h testing. The CH₄ concentration at the reactor exhaust also
6 increased from around 3 to over more than 20 mL min⁻¹. The total increase in CO₂ and CH₄ flow rate
7 was the same as the decrease in CO flow. The decrease in the hydrogen flow rate was related to the
8 CO decrease (2.5:1) and to the CO₂ and CH₄ increase (also 2.5:1). That was close to the stoichiometry
9 of the steam reforming reaction. This suggests that steam reforming is the major reaction in the
10 reforming zone of the reactor. Deactivation of the tested catalyst affected the reforming activity of
11 steam and dry reforming reactions. The possible reason for deactivation of the noble metal catalyst
12 tested was coke deposition. However, even after 1,000 h, the CH₄ concentration was below 1%, as
13 shown in Figure 5. CH₄ conversion decreased from 99 to 94% after 1,000 h operation (Figure 6). With
14 this rate of degradation in catalyst activity, the reactor should operate with high efficiency for a
15 minimum of 5,000 h. No oxygen was observed at the reactor exhaust for all tested cases. In partial
16 oxidation, oxygen is consumed in the first few millimeters of the catalyst bed by surface reactions
17 [18].

18
19 Figure 7 shows SEM images of the AB10 catalyst after the 1,000 h reaction experiment. The surface
20 of the catalyst particles becomes smoother after 1,000 h caused by sintering, except at the reactor
21 inlet where particles were covered by coke flakes (Figure 7a-b). On the surface of the catalyst
22 particles after the reaction debris of Fe from oxidation of the stainless-steel reactor was were
23 visible, on the surface of the catalyst particles after the reaction, due caused by the size of the
24 reactor (10 mm ID). The structure of deposited coke at the reactor inlet differed from the rest of the
25 reactor. At the inlet, coke had a structure of flakes (Figure 7b-c) agglomerated in big particles. The
26 catalyst in the middle of the reactor and at the exhaust was coated with small coke particles equally
27 distributed on the catalyst surface (Figure 7e-f).

28 The deposited coke is a significant component of catalyst deactivation. Deposited carbon along the
29 catalyst bed was analyzed by TGA. The coke deposition was much lower than expected. Initial-Early
30 results [5] for the AB10 catalyst suggested that lack of oxygen leads to coke formation on the CPOX
31 catalyst. The used CH₄:air molar ratio of 1:2.6 presenter in this report is close to stoichiometric and
32 could result in high coke deposition on the CPOX catalyst. However, a lower GHSV with higher
33 reaction temperature and a different catalyst form (spheres) improved resistance to coke
34 deposition. The amount of deposited coke decreased with the catalyst length (Table 2). The inlet is
35 the most active part of the catalyst bed. Beretta et al. [19] reported that 93% of methane can be
36 converted within the first 5 mm from the catalyst inlet during partial oxidation. Higher coke
37 deposition in the inlet zone was detected despite the fact that presence of oxygen should prevent
38 this. This might be explained by different type of deposited coke with the inlet displaying the
39 graphitic type, whereas-while the amorphous type prevailed further downstream the reactor. The
40 characteristic of deposited coke changed along the catalyst bed. For samples of the catalyst from the
41 reactor inlet, the change of mass at 680°C was caused by coke oxidation. The high oxidation
42 temperature suggests graphite-like carbon. However, samples from the middle had a change of mass
43 at 100-150°C caused by moisture removal and a slow steady linear reduction of mass between 300
44 and 1,000°C. Samples of the catalyst from the reactor outlet (after moisture removal at 100-150°C)
45 had a slow linear change of mass between 300 and 600°C, after that temperature the mass was
46 stable. This suggests, that at the bed exhaust soft carbon was deposited (probably on the metal
47 sites) and mixed graphite and soft coke deposited in the middle of the reactor. Shamsi et al. [20]
48 suggested that coke formed on the support is less reactive than coke deposited on metal sites. This
49 may suggest that oxygen present in the reactant gas mixture at the catalyst bed inlet oxidizes
50 hydrogen from the deposited coke making it more graphitic. The slow deactivation of the catalyst
51 with time can be related to the detected coke deposition. Coke deposition decreased with the
52 catalyst length. The color of the catalyst changed after the reaction. Fresh catalyst was brown. After
53 1,000 h of partial oxidation at 750°C, all particles of the catalyst at the reactor inlet (up to 2 cm from
54 inlet) turned white, and particles in the middle and at the outlet black.
55
56
57
58
59
60

The catalyst deactivation was caused by coke deposition combined with sintering. During partial oxidation, there is always a hot-spot formation at the reactor inlet. The hot-spot formation has been reported^[17, 19] to result in progressive loss of the catalyst activity that might result in a faster deactivation of the catalyst. Such loss strongly influences the rate of methane reforming reactions. According to literature^[17], increase in the particle size of noble metal is the most probable reason for the decrease in partial oxidation performance during long time tests. Noble metal sintering affects reforming reactions Eqs. (4)- and (5) but has a lesser effect on oxidation Eqs. (1)-and (2)^[17]. The AB10 is a noble metal catalyst and it can be regenerated by coke oxidation. The procedure for cyclic oxidation to guarantee the long-term operation is still under investigation. The regeneration temperature and time is limited by the portable application of the tested system. TPO analyses of the catalyst used suggests that the regeneration temperature should be above 600°C; however, it should be below system operation temperature. To prevent coke accumulation in long-term operation, Lee et al.^[8] suggested the cyclic operation of several hours of partial oxidation with few minutes of air oxidation. The cyclic operation can reduce the rate of catalyst deactivation. However, for a system where reformat is connected directly to an SOFC, that solution is not practical. The presented results are based on simulation of LNG. In the final system, the low fuel temperature (down to -160°C) will reduce the catalyst activity at the reformer inlet and will lead to a smoother temperature profile. Fuel unconverted on the catalyst will be afterward converted on the anode. That can lead to a cooling effect on the SOFC fuel inlet and is currently being studied. The investigation of fuel dilution by N₂ from partial oxidation is also still ongoing. The obtained results suggest that the final system control needs a mechanism that will stop the flow of air in case of problems with fuel supply to prevent anode oxidation.

4 Conclusion

The performance of a small reforming system for a 100 W SOFC system was evaluated. The catalyst AB10 was analyzed under various reaction temperatures and CH₄:air molar ratios. Although the amount of deposited coke was small, after 1,000 hours of operation the catalyst slowly deactivated with the decrease in CH₄ conversion from 99 to 94% after 1,000 hours of operation. The demonstrated performance of the CPOX reformer confirmed the potential for application of the proposed reformer in an auxiliary power system. It is expected, that the reformer tested in this study will be integrated with a 100 W SOFC system, targeting a market for auxiliary power systems for LNG-powered trucks.

Acknowledgments

The results are part of the SAFARI project funded under Europe's Fuel Cell and Hydrogen Joint Undertaking (FCH JU), Grant Agreement No.325323. The Consortium gratefully acknowledges the support of the FCH JU.

References

- [1] T. Wilberforce, A. Alaswad, A. Palumbo, M. Dassisti, A. G. Olabi, *Int. J. Hydrogen Energy* **2016**, *41*, 16509-16522.
- [2] J. M. Ogden, can be fund under <http://www.afdc.energy.gov/pdfs/31948.pdf>, **2002**, pp. 1-52.
- [3] P. Aguiar, D. Chadwick, L. Kershenbaum, *Chem. Eng. Sci.* **2002**, *57*, 1665-1677.
- [4] Q. Fang, L. Blum, P. Batfalsky, N. H. Menzler, U. Packbier, D. Stolten, *Int. J Hydrogen Energy* **2013**, *38*, 16344-16353.
- [5] A. J. Majewski, A. Dhir, *J. Electrochem. Soc.* **2016**, *163*, F272-F277.
- [6] H.-S. Wang, K.-Y. Huang, Y.-J. Huang, Y.-C. Su, F.-G. Tseng, *Appl. Energy* **2015**, *138*, 21-30.
- [7] T. Aicher, J. Full, A. Schaadt, *Int. J. Hydrogen Energy* **2009**, *34*, 8006-8015.

- [8] S. Lee, G. Keskar, C. Liu, W. R. Schwartz, C. S. McEnally, J.-Y. Kim, L. D. Pfefferle, G. L. Haller, *Appl. Catal. B* **2012**, *111–112*, 157-164.
- [9] aA. A.-S. Saleh, *Open Catal. J.* **2013**, *6*, 17-28; bQ. Zhu, X. Zhao, Y. Deng, *J. Nat. Gas Chem.* **2004**, *13*, 191-203; cB. C. Enger, R. Lødeng, A. Holmen, *Appl. Catal. A*: **2008**, *346*, 1-27.
- [10] aE. Stefana, F. Marciano, M. Alberti, *J. Loss Prev. Process Ind.* **2016**, *39*, 39-58; bQ. Tang, J. Fu, J. Liu, F. Zhou, Z. Yuan, Z. Xu, *Appl. Therm. Eng.* **2016**, *103*, 1351-1361; cO. Schinas, M. Butler, *Ocean Eng.* **2016**, *122*, 84-96.
- [11] E. Graham, A. Kenbar, *Flow Meas. Instrum.* **2015**, *44*, 79-88.
- [12] ALMUS AG, can be fund under <http://www.almus-ag.ch/>, **2016**.
- [13] aU. Bossel, *ECS Trans.* **2015**, *68*, 193-199; bU. Bossel, in *12th European SOFC and SOE forum*, Lucerne, **2016**.
- [14] A. J. Majewski, A. Dhir, *ECS Trans.* **2015**, *68*, 2189-2198.
- [15] aP. D. F. Vernon, M. L. H. Green, A. K. Cheetham, A. T. Ashcroft, *Catal. Lett.* **1990**, *6*, 181-186; bV. Dal Santo, C. Mondelli, V. De Grandi, A. Gallo, S. Recchia, L. Sordelli, R. Psaro, *Appl. Catal. A* **2008**, *346*, 126-133.
- [16] aS. Kumar, S. Kumar, J. K. Prajapati, *Int. J. Hydrogen Energy* **2009**, *34*, 6655-6668; bJ. E. P. Navalho, I. Frenzel, A. Loukou, J. M. C. Pereira, D. Trimis, J. C. F. Pereira, *Int. J. Hydrogen Energy* **2013**, *38*, 6989-7006.
- [17] E. Verlato, S. Barison, S. Cimino, F. Dergal, L. Lisi, G. Mancino, M. Musiani, L. Vázquez-Gómez, *Int. J. Hydrogen Energy* **2014**, *39*, 11473-11485.
- [18] A. Raoufi, S. Kapadia, J. C. Newman lii, *Comput. Chem. Eng.* **2016**, *93*, 266-283.
- [19] A. Beretta, A. Donazzi, D. Livio, M. Maestri, G. Groppi, E. Tronconi, P. Forzatti, *Catal. Today* **2011**, *171*, 79-83.
- [20] A. Shamsi, J. P. Baltrus, J. J. Spivey, *Appl. Catal. A* **2005**, *293*, 145-152.

Reference List

- [1] T. Wilberforce, A. Alaswad, A. Palumbo, M. Dassisti, A. G. Olabi, *International Journal of Hydrogen Energy* **2016**, *41*, 16509-16522.
- [2] J. M. Ogden, Princeton University <http://www.afdc.energy.gov/pdfs/31948.pdf>, **2002**, pp. 1-52.
- [3] P. Aguiar, D. Chadwick, L. Kershenbaum, *Chemical Engineering Science* **2002**, *57*, 1665-1677.
- [4] Q. Fang, L. Blum, P. Batfalsky, N. H. Menzler, U. Packbier, D. Stolten, *International Journal of Hydrogen Energy* **2013**, *38*, 16344-16353.
- [5] A. J. Majewski, A. Dhir, *Journal of The Electrochemical Society* **2016**, *163*, F272-F277.
- [6] H. S. Wang, K. Y. Huang, Y. J. Huang, Y. C. Su, F. G. Tseng, *Applied Energy* **2015**, *138*, 21-30.
- [7] T. Aicher, J. Full, A. Schaadt, *International Journal of Hydrogen Energy* **2009**, *34*, 8006-8015.
- [8] S. Lee, G. Keskar, C. Liu, W. R. Schwartz, C. S. McEnally, J.-Y. Kim, L. D. Pfefferle, G. L. Haller, *Applied Catalysis B: Environmental* **2012**, *111–112*, 157-164.
- [9] aA. A.-S. Saleh, *The Open Catalysis Journal* **2013**, *6*, 17-28; bQ. Zhu, X. Zhao, Y. Deng, *Journal of Natural Gas Chemistry* **2004**, *13*, 191-203; cB. C. Enger, R. Lødeng, A. Holmen, *Applied Catalysis A: General* **2008**, *346*, 1-27.
- [10] aE. Stefana, F. Marciano, M. Alberti, *Journal of Loss Prevention in the Process Industries* **2016**, *39*, 39-58; bQ. Tang, J. Fu, J. Liu, F. Zhou, Z. Yuan, Z. Xu, *Applied Thermal Engineering* **2016**, *103*, 1351-1361; cO. Schinas, M. Butler, *Ocean Engineering* **2016**, *122*, 84-96.
- [11] E. Graham, A. Kenbar, *Flow Measurement and Instrumentation* **2015**, *44*, 79-88.
- [12] Vol. 2016, <http://www.almus-ag.ch/>, **2016**.
- [13] aU. Bossel, *ECS Transactions* **2015**, *68*, 193-199; bU. Bossel, in *12th European SOFC and SOE forum*, Lucerne, **2016**.
- [14] A. J. Majewski, A. Dhir, *ECS Transactions* **2015**, *68*, 2189-2198.

- 1
2
3 [15] aP. D. F. Vernon, M. L. H. Green, A. K. Cheetham, A. T. Ashcroft, *Catal Lett* **1990**, *6*, 181-186;
4 bV. Dal Santo, C. Mondelli, V. De Grandi, A. Gallo, S. Recchia, L. Sordelli, R. Psaro, *Applied*
5 *Catalysis A: General* **2008**, *346*, 126-133.
- 6 [16] aS. Kumar, S. Kumar, J. K. Prajapati, *International Journal of Hydrogen Energy* **2009**, *34*,
7 6655-6668; bJ. E. P. Navalho, I. Frenzel, A. Loukou, J. M. C. Pereira, D. Trimis, J. C. F. Pereira,
8 *International Journal of Hydrogen Energy* **2013**, *38*, 6989-7006.
- 9 [17] E. Verlato, S. Barison, S. Cimino, F. Dergal, L. Lisi, G. Mancino, M. Musiani, L. Vázquez-Gómez,
10 *International Journal of Hydrogen Energy* **2014**, *39*, 11473-11485.
- 11 [18] A. Raoufi, S. Kapadia, J. C. Newman Iii, *Computers & Chemical Engineering* **2016**, *93*, 266-
12 283.
- 13 [19] A. Beretta, A. Donazzi, D. Livio, M. Maestri, G. Groppi, E. Tronconi, P. Forzatti, *Catalysis*
14 *Today* **2011**, *171*, 79-83.
- 15 [20] A. Shamsi, J. P. Baltrus, J. J. Spivey, *Applied Catalysis A: General* **2005**, *293*, 145-152.
- 16
17
18
19
20
21
22
23
24
25
26
27
28
29
30
31
32
33
34
35
36
37
38
39
40
41
42
43
44
45
46
47
48
49
50
51
52
53
54
55
56
57
58
59
60

For Peer Review

Table 1. Overall reactions in the methane partial oxidation system.

ΔH_{298}°	Reaction	Name	Equation Number (as referred in manuscript)
-36 kJ mol ⁻¹	$2CH_4 + O_2 \rightarrow 2CO + 4H_2$	CH ₄ partial oxidation	(1)
-802 kJ mol ⁻¹	$CH_4 + 2O_2 \rightarrow CO_2 + 2H_2O$	CH ₄ combustion	(2)
-41 kJ mol ⁻¹	$CO + H_2O \leftrightarrow CO_2 + H_2$	water gas shift	(3)
+206 kJ mol ⁻¹	$CH_4 + H_2O \leftrightarrow CO + 3H_2$	CH ₄ steam reforming	(4)
+247 kJ mol ⁻¹	$CH_4 + CO_2 \leftrightarrow 2CO + 2H_2$	CH ₄ dry reforming	(5)
-131 kJ mol ⁻¹	$CO + H_2 \leftrightarrow C + H_2O$	CO hydrogenation	(6)
+75 kJ mol ⁻¹	$CH_4 \leftrightarrow C + 2H_2$	CH ₄ cracking	(7)
-173 kJ mol ⁻¹	$2CO \leftrightarrow CO_2 + C$	Boudouard	(8)
-282 kJ mol ⁻¹	$2CO + O_2 \rightarrow 2CO_2$	CO oxidation	(9)
-241 kJ mol ⁻¹	$2H_2 + O_2 \rightarrow 2H_2O$	H ₂ oxidation	(10)

Table 2. Coke deposition on AB10 catalyst - TGA. Catalyst after 1,000 h at 750°C with GHSV 150 L h⁻¹ g_{cat}⁻¹, CH₄:air 1:2.6.

Position in reactor	Coke / mg g _{cat} ⁻¹
Inlet	14.8
Middle	12.8
Outlet	6.0

For Peer Review

Figures captions

Figure 1: A - catalyst HiFUEL AB10 - pellets. B - External reformer (I) for planar cells (designed and manufactured by ALMUS AG).

Figure 2: CH₄ conversion and products yields from different reactors (average from 24 h reaction): (I) - ALMUS reactor; (II) - tubular reactor with ceramic support. Reaction at 700°C, CH₄:air 1:2.4, AB10 catalyst 5 g, CH₄ 724 mL min⁻¹.

Figure 3: Reactor (II) performance at the different reaction temperature (average from 24 h). CH₄:air 1:2.4, 5 g AB10 catalyst, CH₄ gas-in flow 724 mL min⁻¹.

Figure 4: Reactor (II) performance for different CH₄:air ratio 1:x (average from 24 h). Reaction temperature 700°C, 5 g AB10 catalyst CH₄ if flow 724 mL min⁻¹.

Figure 5: Change of gas composition at the reactor (II) outlet with time. Partial oxidation CH₄:air 1:2.6, at 750°C, AB10 catalyst 5 g with GHSV 150 L h⁻¹ g_{cat}⁻¹.

Figure 6: Change in methane conversion with time. Partial oxidation CH₄:air 1:2.6, at 750°C, AB10 catalyst 5 g with GHSV 150 L h⁻¹ g_{cat}⁻¹, reactor (II).

Figure 7: SEM scans of the AB10 spent catalyst after 1,000 h at 750°C with GHSV 150 L h⁻¹ g_{cat}⁻¹, CH₄:air 1:2.6, reactor (I), A-C reactor inlet, D-F reactor exhaust. C and F - EDX carbon mapping of scans B and E respectively.

1
2
3
4
5
6
7
8
9
10
11
12
13
14
15
16
17
18
19
20
21
22
23
24
25
26
27
28
29
30
31
32
33
34
35
36
37
38
39
40
41
42
43
44
45
46
47
48
49
50
51
52
53
54
55
56
57
58
59
60

For Peer Review